VER
Vascular & Endovascular Review

Naloxone Pretreatment Mitigates Secondary Renal Injury Following Hepatic Ischemia-Reperfusion in Rats

Abdelhamid Sayed Abo Bakr[1], Samah Mohammed Mahmoud Abozaid[1], Nashwa Fathy Gamal EL-Tahawy[2], Rania Nady Nour El Deen[1], Medhat Atta Salah[1]

[1]Department of Human Anatomy and Embryology, Faculty of Medicine, Minia University, Minia, Egypt
[2]Department of Histology and Cell Biology, Faculty of Medicine, Minia University, Minia, Egypt

ABSTRACT

Background: Hepatic ischemia–reperfusion (I/R) injury is a major complication of liver surgery and transplantation, often extending its harmful effects to distant organs such as the kidneys. Naloxone, a non-selective opioid receptor antagonist, has shown potential protective properties against I/R-induced tissue damage, but its role in renal protection following hepatic I/R remains unclear.

Objective: This study aimed to investigate the protective effects of naloxone pre-treatment on renal injury induced by hepatic I/R in rats.

Methods: The adult male albino rats (n=40) were subjected to a random division into four experimental cohorts: control, sham-operated, hepatic I/R, and naloxone + I/R.

Hepatic ischemia was induced by occluding the portal triad for 45 minutes, followed by 60 minutes of reperfusion. Serum ALT, AST, urea, and creatinine levels were measured, along with renal malondialdehyde (MDA) and TNF-α levels. Kidney tissues were evaluated histologically (H&E), immunohistochemically (COX-2, NF-κB, and caspase-3), and morphometrically.

Results: Hepatic I/R resulted in significant hepatic and renal dysfunction, oxidative stress, and inflammatory changes, evidenced by elevated serum biomarkers, disrupted renal histology, and increased COX-2, NF-κB, and caspase-3 expression. Naloxone pre-treatment markedly attenuated these alterations, preserving renal architecture, reducing oxidative stress, and lowering inflammatory and apoptotic marker expression.

Conclusion: Naloxone pre-treatment exhibits a protective effect against renal injury secondary to hepatic I/R by mitigating oxidative, inflammatory, and apoptotic pathways. These findings suggest its potential application as an adjuvant therapeutic strategy in liver surgery and transplantation.

KEYWORDS: Saw Palmetto, Beta-Sitosterol, Pygeum Africanum, Phytotherapy, Benign Prostatic Hyperplasia, BPH 2.

How to Cite: Abdelhamid Sayed Abo Bakr, Samah Mohammed Mahmoud Abozaid, Nashwa Fathy Gamal EL-Tahawy, Rania Nady Nour El Deen, Medhat Atta Salah, (2025) Naloxone Pretreatment Mitigates Secondary Renal Injury Following Hepatic Ischemia-Reperfusion in Rats, Vascular and Endovascular Review, Vol.8, No.16s, 51-78.

INTRODUCTION

Ischemia/reperfusion injury (I/RI) is characterized by a series of functional and structural disturbances that occur when blood flow is re-established after a period of ischemia. Although the restoration of circulation is critical for tissue survival, it paradoxically can exacerbate injury, leading to necrosis of irreversibly damaged cells, pronounced cellular edema, and heterogeneous reperfusion within the affected tissue. This disordered reflow, often termed the "No-Reflow Phenomenon." This pathological condition results from a self-perpetuating cycle of vascular, endothelial, and mitochondrial dysfunction, characterized by impaired local perfusion, severe structural disturbances, edema, and other detrimental effects. The development of metabolic disturbances during both the ischemic phase and subsequent reperfusion is now recognized as a major contributor to cellular and tissue damage **(Soares et al., 2019).**

Hepatic ischemia-reperfusion injury (IRI) represents a major challenge during liver surgery, liver preservation for transplantation, and can cause hemorrhagic shock with severe hypoxemia and trauma. **(Pretzsch et al., 2022).** The liver is especially vulnerable to systemic ischemia/reperfusion injury (SI/RI), and prior research has linked hepatic I/RI to mitochondrial dysfunction, the overproduction of reactive oxygen species, and elevated rates of apoptosis **(Zhou et al., 2021).**

Importantly, liver I/R has widespread systemic consequences, potentially impairing the function of distant organs such as the lungs, kidneys, intestines, pancreas, adrenal glands, and heart. These remote organ injuries are believed to be partially driven by oxidative stress and an amplified inflammatory response following reperfusion **(Nastos et al., 2014; Mouratidou et al., 2023).** Acute kidney injury (AKI) represents a major global health challenge, characterized by high morbidity and mortality rates, which has driven extensive research into effective preventive and therapeutic strategies. Among the primary mechanisms underlying AKI, ischemia–reperfusion (I/R) injury plays a pivotal role by inducing profound cellular damage **(Murry et al., 1986).**

Several therapeutic approaches have been explored to mitigate liver ischemia–reperfusion (I/R) injury, including organ

preservation techniques, suppression of reactive oxygen species (ROS) generation, and modulation of immune responses. Among these, organ preservation strategies have yielded the most favorable outcomes. In contrast, pharmacological interventions such as tumor necrosis factor (TNF) inhibitors, corticosteroids, and antioxidants like N-acetylcysteine have generally demonstrated limited or inconsistent protective effects **(Đurašević et al., 2021).** Naloxone, particularly its (Z)-stereoisomer, acts as a stereospecific but non-selective antagonist of the three primary opioid receptors. Interestingly, emerging evidence suggests that naloxone's protective effects may be attributed more to its influence on inflammatory pathways than to its interaction with classical opioid receptors **(van Lemmen et al., 2023)**. Several studies have indicated that naloxone administration can attenuate tissue damage in experimental models of ischemia-reperfusion injury, supporting its potential as a protective agent **(Chen et al., 2016; Wang et al., 2019)**. Opioids, via their receptors, are believed to contribute to the mechanisms underlying I/R injury. Thus, opioid receptor blockade by naloxone may offer a means to mitigate such damage. Despite these insights, the exact role of naloxone in mitigating ischemia–reperfusion (I/R) injury has not been fully elucidated. Therefore, the primary objective of this research was to evaluate the potential of naloxone pretreatment to provide protection against renal damage following hepatic I/R in rats.

MATERIALS AND METHODS

Ethical Approval

The research protocol received ethical approval from the Faculty of Medicine's Ethical Committee at Minia University, in October 2020.

Chemicals

Naloxone hydrochloride was used in the form of NARCAN, a 0.4 mg/ml injectable solution manufactured by SERB Pharmaceuticals, Europe. It was administered intravenously at a dose of 3.0 mg/kg, 30 minutes prior to the induction of ischemia, in accordance with previous research **(Takhtfooladi et al., 2016).**

Experimental Animals

Forty adult male albino rats (200–250 g) were obtained from the university's animal facility. All animals were Specific-Pathogen-Free (SPF) and acclimatized for one week before the experiments. They were housed under standard laboratory conditions in ventilated plastic cages with unrestricted access to food and water.

Experimental Design

The forty rats were randomly allocated into four experimental groups (n=10 per group):

- Group I (Control) (C): received a standard laboratory diet and water without any surgical intervention.
- Group II (Sham-operated) (SC): underwent the full surgical protocol except for hepatic vascular clamping.
- Group III (LIR): subjected to hepatic ischemia/reperfusion (LIR) surgery.
- Group IV (LIR+ naloxone): received intravenous naloxone (3.0 mg/kg) 30 minutes before undergoing the LIR procedure.

Liver Ischemia/Reperfusion Surgical Procedure

The animals were anesthetized with ketamine (50 mg/kg) and xylazine (10 mg/kg) and placed in a supine position on a heating pad maintained at 36–37 °C. Following aseptic preparation, a midline laparotomy (abdominal incision) was performed. Liver ischemia in the LIR and naloxone + LIR groups was induced by clamping the portal triad (the portal vein, hepatic artery, and common bile duct) with an atraumatic microvascular bulldog clamp for 45 minutes. To prevent hypothermia and visceral dehydration, the peritoneal cavity was kept moist with warm saline (37 °C), and the incision was covered with plastic wrap. Following 45-minute ischemic interval, the clamp was released, to allow 60 minutes of reperfusion, consistent with Pringle's maneuver **(Kamel et al., 2015).** Macroscopically, the liver exhibited pallor during the ischemic phase and became visibly congested/bluish upon reperfusion.

Tissue and Sample Collection

Upon completion of the reperfusion period, the rats were immediately euthanized. Blood samples were collected from the descending abdominal aorta and centrifuged at 4000 xg for 10 minutes to obtain serum for liver enzyme and kidney function analysis. The kidneys were harvested, divided and processed as follows: one portion was homogenized in cold saline, then stored at −20°C, and centrifuged at 5000 xg for 15 minutes for subsequent biochemical analyses (MDA and TNF-α). The remaining portion was fixed in 10% neutral-buffered formalin for subsequent histopathological and immunohistochemical processing.

Liver Function Assessment

Levels of Serum alanine transaminase (ALT) and aspartate transaminase (AST) were measured via enzymatic colorimetric assay kits from Biodiagnostic (Cairo, Egypt), strictly adhering to the procedures set by the manufacturer.

Renal Function Assessment

Urea (blood urea nitrogen, BUN) and creatinine concentrations were determined according to enzymatic colorimetric kits from Biodiagnostic (Cairo, Egypt) strictly following the provided guidelines.

Renal Oxidative Stress Markers

Renal lipid peroxidation was assessed by determining malondialdehyde (MDA) levels through the thiobarbituric acid reactive substances (TBARS) method, using 1, 1, 3, 3- tetramethoxypropane as the standard (Buege & Aust, 1978). Tumor necrosis factor-

alpha (TNF-α), a key indicator of inflammatory response, was quantified using an ELISA kit (Elabscience Biotechnology Inc., USA; Cat. No. E-EL-R0019E).

Histopathological Examination

Kidney tissue samples were dissected into small pieces and fixed in 4% formaldehyde for 48 hours. The fixed samples were then processed by graded ethanol dehydration, xylene clearing, and paraffin embedding. Serial 4-µm sections were cut, deparaffinized, and stained with hematoxylin and eosin (H&E) following standard histological procedures **(Suvarna et al., 2018)**.

Histochemical technique: **Periodic Acid–Schiff (PAS) Staining**

Periodic Acid-Schiff (PAS) staining is a histochemical technique used to detect polysaccharides, such as glycogen, mucosubstances, and glycoproteins, in tissues. The procedure begins with formalin-fixed, paraffin-embedded sections (4-5 \mu \text{m} thick), which are first deparaffinized and rehydrated. The tissues are then oxidized with 0.5-1\% periodic acid for 5-10 minutes to generate aldehyde groups from carbohydrate components. After rinsing, the sections are incubated with Schiff's reagent for 10-15 minutes, leading to a distinctive magenta coloration where aldehydes are present. A tap water rinse enhances color development. PAS staining is valuable for highlighting basement membranes, glomerular structures, brush borders, glycogen deposits, and fungal organisms in histopathological analysis **(Carson et al., 2015).**

Immunohistochemical Analysis

Paraffin-embedded renal sections (4 µm) were mounted on positively charged slides, deparaffinized, and rehydrated. Antigen retrieval was achieved via 0.1%trypsin digestion for 15 minutes at 37 °C, followed by a wash with phosphate-buffered saline (PBS). Endogenous peroxidase activity was blocked with 3% hydrogen peroxide, followed by the application of an Ultra V Block to prevent nonspecific background staining. Sections were incubated overnight in a humid chamber with primary antibodies targeting (i) COX-2 (inflammation marker), (ii) NF-κB p65 (rabbit polyclonal, Cat. No BS-20159R, Bios Antibodies; 1:100), and (iii) caspase-3 (rabbit polyclonal, Cat No PA1-29157, Thermo Fisher Scientific; 1:100) to evaluate inflammatory and apoptotic activity **(Maae et al., 2011).**

Morphometric Evaluation

The immuno-positive area fraction for COX-2, NF-κB, and caspase-3 cells was calculated as a percentage by examining ten non-overlapping microscopic fields per tissue section. Analysis was performed using ImageJ 22 software under an Olympus CX41 light microscope at 400× magnification.

Statistical Analysis

All quantitative data, including serum ALT, AST, LDH, urea, creatinine, and renal MDA and TNF-α levels, were presented as mean ± standard error of the mean (SEM). Statistical differences between groups were assessed using one-way ANOVA, followed by Tukey–Kramer post hoc test, using GraphPad Prism (version 9) software. A p-value of < 0.05 was considered statistically significant.

RESULTS

Biochemical results:

Effect of Naloxone on LIR-Induced Hepatic Dysfunction

In terms of hepatic function, the sham-operated (SC) group exhibited a non-significant elevation in serum alanine aminotransferase (ALT) levels compared to the control (C) group ($p = 0.3455$). However, a statistically significant increase in serum aspartate aminotransferase (AST) level was observed in the SC group relative to the C group ($p = 0.0013$). Rats subjected to liver ischemia-reperfusion (LIR) showed markedly elevated serum ALT and AST levels compared to both the C and SC groups ($p < 0.0001$ for both). Treatment with naloxone in the LIR + naloxone group significantly reduced these enzymes levels compared to the untreated LIR group. Nevertheless, enzyme levels in the naloxone-treated group remained significantly higher than those in the C and SC groups (all $p < 0.0001$) (Tables 1, 2 and Histograms 1, 2)

Effect of Naloxone on LIR-Induced Renal Dysfunction

Assessment of renal function revealed that the SC group exhibited a significant increase in serum urea levels compared to the C group ($p < 0.0001$), while serum creatinine levels remained statistically non-significant ($p = 0.5316$). The LIR group demonstrated a significant increase in both serum urea and creatinine levels compared to C and SC groups ($p < 0.0001$ for both). Naloxone administration in the LIR + naloxone group significantly attenuated these levels relative to the LIR group but did not restore them to baseline levels, as they remained significantly higher than in the C and SC groups (all $p < 0.0001$) (Tables 3, 4 and Histograms 3, 4).

The impact of Naloxone on LIR-induced renal malondialdehyde (MDA) (nmol\mg) and renal tumor necrosis factor-alpha (TNF-α) (pg/mg):

Regarding oxidative stress and inflammation markers, the SC group exhibited a non-significant increase in renal malondialdehyde (MDA) levels compared to the C group ($p = 0.8171$), but a significant increase in tumor necrosis factor-alpha (TNF-α) levels ($p = 0.048$). The LIR group displayed highly significant increases in both renal MDA and TNF-α levels compared to C and SC groups ($p < 0.0001$). Naloxone treatment significantly reduced these markers in the LIR + naloxone group compared to the LIR group; however, the values remained significantly elevated compared to C and SC groups (all $p < 0.0001$) (Tables 5, 6 and Histograms 5, 6).

Hematoxylin and Eosin results:

The Control group (C) and Sham-operated group (SC):

Examination of H&E-stained sections in the control group (Fig. 1) and in sham operated group (Fig. 3) showed normal histological structure of the renal cortex demonstrating renal corpuscles, proximal (PCTs) and distal (DCTs) convoluted tubules. These renal corpuscles were formed of lobulated capillary tufts (the glomeruli), which were surrounded by Bowman's capsule (consisting of a parietal layer and a visceral layer). A patent urinary space (Bowman's space) was visible between these two layers. The renal corpuscles were surrounded by PCTs and DCTs (Figs. 2, 4).

The PCTs occupied the main bulk of the renal cortex. They exhibited variable shapes with narrow lumina, and were lined by high cuboidal (pyramidal) cells with indistinct cell boundaries. The cytoplasm was acidophilic and granular with basal rounded vesicular nuclei (Figs. 2, 4).

The DCTs appeared with larger, regular, and distinct lumina. They were lined with low cuboidal cells featuring pale acidophilic cytoplasm and rounded nuclei (Figs. 2, 4).

Liver Ischemia-Reperfusion group (LIR group):

Examination of H&E-stained sections obtained from the LIR group revealed patchy and variable histological changes in the renal cortices, characterized by significant glomerular and tubulointerstitial injury. Some areas exhibited distorted renal corpuscles that were shrunken and atrophied, while others appeared hypertrophied with narrowing of their bowman's spaces. Most renal corpuscles appeared congested (Figs. 5,6).

Congestion of peritubular capillaries and interstitial hemorrhage was also observed in some sections (Figs.6).

Marked tubular distortion was observed in several renal cortical sections. Tubular epithelial cells exhibited marked vacuolation and desquamation into the tubular lumina accompanied by cellular debris accumulation. Some cells exhibited nuclear ghosting (pyknosis/ karyolysis) and loss of cytoplasm, while others showed flattening of the epithelial lining with reduction in cell height (Figs.6,7).

Some tubular lumina showed homogeneous eosinophilic hyaline casts (Fig.7). Additionally, an interstitial inflammatory infiltrate, composed mostly of lymphocytes, was noted (Fig.6).

Liver Ischemia-Reperfusion and Naloxone group (LIR + naloxone group):

This group demonstrated an amelioration of the previously mentioned pathological findings, as evidenced by a reduction in histological changes compared to the LIR group.

The renal cortex showed a marked restoration of its architecture (Fig. 8). The renal corpuscles exhibited a near-normal size and morphology, showing significant recovery from the atrophy noted in the LIR group, although some congestion of glomerular capillaries persisted. Peritubular congestion was decreased, and interstitial hemorrhage was absent.

However, some intraluminal hyaline casts were still observed. Most PCTs and DCTs retained their near-normal epithelial lining, with no cellular casts observed (Fig. 9).

Periodic acid-Schiff (PAS) results:

The control group (C-group):

Renal cortical tissues of this group showed positive PAS reactions in the basement membranes of intact glomerular capillaries, the parietal layer of bowman's capsules and the PCT and DCT cells. Positive PAS reactivity was also observed in the intact apical brush borders of the PCT and DCT cells (Fig.10).

The sham operated group (SC-group):

Sections of the renal cortex of the SC-group showed a PAS-positive reaction was nearly identical to that of C-group in the basement membranes of intact glomerular capillaries, parietal layer of bowman's capsule and the PCT and DCT cells. However, a positive reaction was observed in PCT and DCT apical brush borders with only few, minor focal interruptions noted in the glomerular basement membranes (Fig.11).

Liver ischemia reperfusion group (LIR group):

PAS-stained sections of the renal cortex from the LIR group demonstrated a significantly reduced PAS reaction. This reduction was manifested as partial or complete effacement (loss) of the brush border in the majority of distorted tubules. Furthermore, the basement membranes of renal tubules and glomerular capillaries appeared fragmented and attenuated (thinned) in several areas (Fig.12).

Liver ischemia reperfusion-naloxone group (LIR+ naloxone group):

Sections of the renal cortex of the LIR+ naloxone group demonstrated a significantly preserved PAS reaction in the majority of the brush borders of the PCTs and DCTs. The basement membranes of glomerular capillaries, parietal layer of Bowman's capsules, and the PCTs and DCTs cells appeared continuous and structurally intact. Only few renal tubules exhibited a diminished PAS reaction associated with focal interruptions of their brush borders (Fig.13).

IMMUNOHISTOCHEMICAL STUDY:

A. Immunohistochemical Study of Cyclooxygenase-2 (COX-2) Expression:

The positive immunoreactivity for COX-2 appeared as brown cytoplasmic coloration in the reactive cells.

The Control Group (C-group):

Control group rat renal sections stained for COX-2 showed negative cytoplasmic immunoreactivity in the glomerular, proximal convoluted tubule (PCT), and distal convoluted tubule (DCT) cells (Fig. 14).

The Sham-Operated Group (SC group):
This group showed negative COX-2 immunoreactivity in glomerular and tubular cells, similar to the C-group (Fig. 15).

Liver Ischemia-Reperfusion (LIR) Group:
Sections from this group displayed numerous, deeply stained COX-2 cytoplasmic immunoreactive cells in the glomeruli, PCTs, and DCTs. This was in contrast to the control groups, which showed only faint positive cytoplasmic immunoreactivity in some glomerular and tubular cells (Figs. 16, 17).

Liver Ischemia-Reperfusion and Naloxone (LIR + Naloxone) Group:
There was an apparent decrease in COX-2 immunoreactivity in this group compared to the LIR group. Most glomerular, PCT, and DCT cells showed faint positive cytoplasmic immunoreactivity (Fig. 18).

B. Immunohistochemical Study of Nuclear Factor Kappa B (NF-κB) Expression:
The positive immunoreactivity for NF-κB appeared as brown cytoplasmic coloration in the reactive cells.
The Control Group (C-group):
Control group rat renal sections stained for NF-κB showed negative cytoplasmic immunoreactivity in the glomerular, PCT, and DCT cells (Fig. 19).

The Sham-Operated Group (SC group):
This group showed negative NF-κB immunoreactivity in glomerular and tubular cells, similar to the C-group, except for faint cytoplasmic expression in a few tubular cells (Fig. 20).

Liver Ischemia-Reperfusion (LIR) Group:
Sections from this group displayed numerous, deeply stained NF-κB cytoplasmic immunoreactive cells in PCT and DCT cells. Compared to the C-group, faint positive cytoplasmic immunoreactivity was also observed in other glomerular and tubular cells (Fig. 21).

Liver Ischemia-Reperfusion and Naloxone (LIR + Naloxone) Group:
There was an apparent decrease in NF-κB immunoreactivity in this group compared to the LIR group. Some glomerular, PCT, and DCT cells showed faint positive cytoplasmic immunoreactivity, while other cells showed negative immunoreactivity (Fig. 22).

C. Immunohistochemical study of the rat kidney using activated (cleaved) Caspase-3 Expression:
Positive immunoreactivity for activated caspase-3 was observed as brown coloration in the cytoplasm and/or nuclei of the immunoreactive cells.
The Control Group (C-group):
No detectable immunolabeling for activated caspase-3 was found in the renal tissue sections of the control group (Fig. 23).

The Sham-operated Group (SC-group):
The SC-group sections showed negative immunoreactivity for activated caspase-3 in the renal sections, similar to the C-group (Fig. 24).

Liver Ischemia/Reperfusion Group (LIR group):
There was increased immunoreactivity for activated caspase-3 in renal glomerular cells and renal tubular cells. The cells of the renal corpuscle showed positive cytoplasmic immunoreaction for activated caspase-3. Additionally, tubular cells exhibited positive cytoplasmic and nuclear immunoreactions (Fig. 25).

Liver Ischemia/Reperfusion-Naloxone Group (LIR + Naloxone Group):
There was an apparent reduction in the immunoreactivity for activated caspase-3 when compared to the LIR group. Faint cytoplasmic expression of activated caspase-3 was observed in glomerular and renal tubular cells, with mild or absent immunolabeling of activated caspase-3 in other cells (Fig. 26).

Morphometric Evaluation (Analysis)

A. Morphometric Analysis of Cyclooxygenase-2 (COX-2) :
Morphometric analysis revealed that the SC-group exhibited an insignificant increase in renal COX-2 immunoreactivity compared to the C-group ($p=0.999$). The LIR group showed a significant increase in renal COX-2 immunoreactivity compared to both the C and SC groups (both $p<0.0001$). However, the administration of naloxone in the LIR+ naloxone group significantly reduced COX-2 immunoreactivity compared with the LIR group ($p<0.0001$). Conversely, this reduced expression significantly increased compared with the C and SC groups (both $p<0.0001$) (Table 7, Histogram 7).

B. Morphometric Analysis of Nuclear Factor Kappa B (NF-κB) Expression:
Morphometric analysis revealed that the SC-group exhibited an insignificant increase in NF-κB immunoreactivity in renal tissue compared to the C-group ($p=0.999$). The LIR group demonstrated a significant increase in renal NF-κB

immunoreactivity when compared to both the C and SC groups (both p<0.0001). However, the administration of naloxone in the LIR+ naloxone group significantly reduced NF-κB immunoreactivity compared with the LIR group (p<0.0001). Conversely, this reduced expression remained significantly increased compared with the C and SC groups (both p<0.0001) (Table 8, Histogram 8).

C. Morphometric Analysis of the rat kidney using activated (cleaved) Caspase-3:

Morphometric analysis revealed that the SC-group exhibited an insignificant increase in caspase-3 immunoreactivity in renal tissue compared to the C-group (p=0.999). The LIR group demonstrated a significant increase in caspase-3 immunoreactivity when compared to both the C and SC groups (both p<0.0001). However, the administration of naloxone in the LIR+ aloxone group significantly reduced caspase-3 immunoreactivity compared with the LIR group (p<0.0001). Conversely, this reduced expression remained significantly elevated compared with the C and SC groups (both p<0.0001) (Table 9, Histogram 9).

DISCUSSION

1. The Main Conclusion and Functional Confirmation

Acute Kidney Injury (AKI) following procedures that induce hepatic IR is a severe complication that significantly increases morbidity and mortality **(Lee et al., 2009)**.

This study aimed to investigate the protective effects of Naloxone pretreatment against Acute Kidney Injury (AKI) secondary to remote hepatic Ischemia/Reperfusion (I/R) injury in rats. The findings unequivocally demonstrate that Naloxone significantly mitigates renal dysfunction and morphological damage, establishing its potential as a renoprotective agent in this clinically relevant setting.

The severe renal injury observed in the LIR group was confirmed by highly significant elevations in serum Creatinine and Urea ($p < 0.0001$), reflecting profound functional impairment. Conversely, Naloxone pretreatment dramatically attenuated these increases, restoring these functional biomarkers close to the levels of the control groups. Histopathological analysis (H&E and PAS) further corroborated the functional data, showing marked tubular degeneration, necrosis (as noted by pyknosis/karyolysis), and brush border loss in the LIR group, which were significantly reduced or even reversed in the LIR + Naloxone group **(Gao et al., 2024).**

2. Mechanistic Insight: The Role of Oxidative Stress, Inflammation, and Apoptosis

To elucidate the mechanism underlying Naloxone's protective action, we investigated key molecular pathways known to mediate the liver-kidney crosstalk **(Rad et al., 2024).**

Oxidative Stress Mitigation: Hepatic I/R is known to generate vast amounts of reactive oxygen species (ROS), leading to systemic oxidative stress and subsequent remote organ damage **(Nastos et al., 2014)**. Malondialdehyde (MDA), a terminal byproduct of lipid peroxidation, is utilized as one of the most common and reliable biomarkers for assessing the extent of oxidative stress **(Singh et al., 2014; Jadoon et al., 2017**). Elevated MDA levels correlate directly with the severity of oxidative damage and impaired antioxidant capacity in various pathological states, including IR injury **(Khoubnasabjafari et al., 2015)**. Therefore, quantifying MDA levels was a crucial component of this study for assessing the severity of IR-induced damage.

Our data confirmed this, showing a significant increase in renal Malondialdehyde (MDA) levels (a biomarker for lipid peroxidation) in the LIR group. The ability of Naloxone to significantly reduce renal MDA indicates that its renoprotection involves potent antioxidant activity and preservation of cellular membranes against ROS attack, consistent with prior findings on Naloxone in I/R injury models **(Takhtfooladi et al., 2016).**

Suppression of Inflammatory Signaling: Inflammation is a critical driver of remote AKI. Our results showed profound activation/translocation of the master regulator of inflammation, NF-kB, and its downstream target, COX-2, alongside a significant increase in the pro-inflammatory mediator TNF-alpha. Crucially, the administration of Naloxone significantly suppressed the expression of NF-kB and COX-2 ($p < 0.0001$ for both). This result strongly suggests that Naloxone exerts its anti-inflammatory effect by inhibiting the NF-kB signaling pathway, thereby interrupting the systemic inflammatory cascade that transmits injury from the liver to the kidney **(Wang et al., 2019)**.

Anti-Apoptotic Effect: Furthermore, LIR injury triggered significant programmed cell death, as confirmed by the strong immunohistochemical expression of activated Caspase-3. The significant decrease in Caspase-3 expression in the Naloxone group confirms the drug's role in preserving renal tubular cell viability by inhibiting the intrinsic apoptotic pathway. This anti-apoptotic action is a key mechanism identified for Naloxone in other models of ischemic injury **(Wang et al., 2019)**.

3. Comparison with Existing Literature and Novelty

The phenomenon of hepatic I/R-induced AKI is a major clinical concern in transplantation and liver surgery [Ref. 2.4]. Our findings align with the established knowledge that this remote damage is driven by circulating inflammatory and oxidative mediators **(Rad et al., 2024)**.

The novelty of this study lies in the comprehensive, multi-target validation of Naloxone's role in this specific remote injury model. Naloxone, an opioid receptor antagonist, is suggested to possess protective properties, possibly by blocking specific opioid receptors (ORs) that typically exacerbate inflammation **(Gao et al., 2024)**. Our results demonstrate that Naloxone's protective effect is mediated by the simultaneous targeting of oxidative stress, NF-kB-dependent inflammation, and apoptosis. This

comprehensive, multi-pathway inhibition makes Naloxone a highly promising therapeutic candidate, particularly since its mechanism goes beyond simple OR antagonism to include direct anti-inflammatory signaling **(Lin et al., 2017)**.

4. Conclusion and Future Perspectives

In conclusion, Naloxone pretreatment effectively mitigated secondary AKI following hepatic I/R in rats. This protection is mediated by its capacity to reduce oxidative stress, inhibit the NF-kB inflammatory pathway, and suppress Caspase-3 dependent apoptosis. These findings suggest that Naloxone could represent an adjuvant therapeutic strategy to be considered prior to major liver surgeries or transplantation to significantly reduce the risk of postoperative AKI. Future studies should focus on identifying the specific OR subtypes involved in this renoprotection and evaluating its efficacy in a clinical setting.

CONCLUSION

LIR not only induces marked hepatic damage but also triggers systemic oxidative stress, and significant renal injury, as evidenced by biochemical, histopathological, and immunohistochemical alterations. Administration of naloxone demonstrated a protective effect against LIR-induced multi-organ injury, likely through its anti-inflammatory, anti-apoptotic, and antioxidant properties. These findings highlight naloxone's potential therapeutic role in mitigating ischemia-reperfusion-related systemic complications.

FUTURE PERSPECTIVES AND RECOMMENDATIONS

- Future studies should investigate the specific signaling pathways involved in naloxone's anti-inflammatory and anti-apoptotic effects.
- Dose-response studies are recommended to identify the most effective and safest therapeutic concentration of naloxone.
- Longer reperfusion intervals should be evaluated in further studies to assess the durability of naloxone's protective effects.
- The current findings should be validated in larger animal models or early-phase clinical studies to explore their translational potential.
- Comparative studies of naloxone against established antioxidants or anti-inflammatory agents are needed to benchmark its efficacy.

REFERENCES

1. Soares RO, Losada DM, Jordani MC, Évora P, Castro-e-Silva O. Ischemia/reperfusion injury revisited: an overview of the latest pharmacological strategies. International journal of molecular sciences. 2019 Oct 11;20(20):5034.
2. Pretzsch E, Nieß H, Khaled NB, Bösch F, Guba M, Werner J, Angele M, Chaudry IH. Molecular mechanisms of ischaemia-reperfusion injury and regeneration in the liver-shock and surgery-associated changes. International journal of molecular sciences. 2022 Oct 26;23(21):12942.
3. Zhou H, Li L, Sun H, Li H, Wu Y, Zhang X, Zhang J. Remote ischemic preconditioning attenuates hepatic ischemia/reperfusion injury after hemorrhagic shock by increasing autophagy. International Journal of Medical Sciences. 2021 Jan 1;18(4):873.
4. Nastos C, Kalimeris K, Papoutsidakis N, Tasoulis MK, Lykoudis PM, Theodoraki K, Nastou D, Smyrniotis V, Arkadopoulos N. Global consequences of liver ischemia/reperfusion injury. Oxidative medicine and cellular longevity. 2014;2014(1):906965.
5. Mouratidou C, Pavlidis ET, Katsanos G, Kotoulas SC, Mouloudi E, Tsoulfas G, Galanis IN, Pavlidis TE. Hepatic ischemia-reperfusion syndrome and its effect on the cardiovascular system: The role of treprostinil, a synthetic prostacyclin analog. World Journal of Gastrointestinal Surgery. 2023 Sep 27;15(9):1858.
6. Murry CE, Jennings RB, Reimer KA. Preconditioning with ischemia: a delay of lethal cell injury in ischemic myocardium. Circulation. 1986 Nov;74(5):1124-36.
7. Đurašević S, Stojković M, Sopta J, Pavlović S, Borković-Mitić S, Ivanović A, Jasnić N, Tosti T, Đurović S, Đorđević J, Todorović Z. The effects of meldonium on the acute ischemia/reperfusion liver injury in rats. Scientific Reports. 2021 Jan 14;11(1):1305.
8. van Lemmen M, Florian J, Li Z, van Velzen M, van Dorp E, Niesters M, Sarton E, Olofsen E, van der Schrier R, Strauss DG, Dahan A. Opioid overdose: limitations in naloxone reversal of respiratory depression and prevention of cardiac arrest. Anesthesiology. 2023 Aug 8;139(3):342-53.
9. Chen Y, Heng W, Hao M, Li L, Xu M. Therapeutic Effects of Naloxone Combined with Edaravone on Elderly Patients with Acute Cerebral Infarction. International Journal of Pharmacology. 2022 Jan 1;18(8):1568-75.
10. Wang X, Sun ZJ, Wu JL, Quan WQ, Xiao WD, Chew H, Jiang CM, Li D. Naloxone attenuates ischemic brain injury in rats through suppressing the NIK/IKKα/NF-κB and neuronal apoptotic pathways. Acta Pharmacologica Sinica. 2019 Feb;40(2):170-9.
11. Takhtfooladi MA, Shahzamani M, Asghari A, Fakouri A. Naloxone pretreatment prevents kidney injury after liver ischemia reperfusion injury. International urology and nephrology. 2016 Jul;48(7):1113-20.
12. Kamel EO, Hassanein EH, Ahmed MA, Ali FE. Perindopril ameliorates hepatic ischemia reperfusion injury via regulation of NF-κB-p65/TLR-4, JAK1/STAT-3, Nrf-2, and PI3K/Akt/mTOR signaling pathways. The Anatomical Record. 2020 Jul;303(7):1935-49.
13. Suvarna KS, Layton C, Bancroft JD. Bancroft's theory and practice of histological techniques E-Book. Elsevier health sciences; 2018 Feb 27.
14. Carson FL, HLADIK C. Histotechnology. A self-instructional text. 2015: American-Society.
15. Maae E, Nielsen M, Steffensen KD, Jakobsen EH, Jakobsen A, Sørensen FB. Estimation of immunohistochemical expression of VEGF in ductal carcinomas of the breast. Journal of Histochemistry & Cytochemistry. 2011 Aug;59(8):750-60.

16. Lee HT, Park SW, Kim M, D D'Agati V. Acute kidney injury after hepatic ischemia and reperfusion injury in mice. Laboratory investigation. 2009 Feb 1;89(2):196-208.
17. Gao S, He Q. Opioids and the kidney: two sides of the same coin. Frontiers in Pharmacology. 2024 Jul 25; 15:1421248.
18. Rad NK, Heydari Z, Tamimi AH, Zahmatkesh E, Shpichka A, Barekat M, Timashev P, Hossein-Khannazer N, Hassan M, Vosough M. Review on kidney-liver crosstalk: pathophysiology of their disorders. Cell Journal (Yakhteh). 2024 Feb 28;26(2):98.
19. Nastos C, Kalimeris K, Papoutsidakis N, Tasoulis MK, Lykoudis PM, Theodoraki K, Nastou D, Smyrniotis V, Arkadopoulos N. Global consequences of liver ischemia/reperfusion injury. Oxidative medicine and cellular longevity. 2014;2014(1):906965.
20. Singh Z, Karthigesu IP, Singh P, Kaur R. Use of malondialdehyde as a biomarker for assessing oxidative stress in different disease pathologies: a review. Iranian Journal of Public Health. 2014;43(Supple 3):7-16.
21. Jadoon S, Malik A. A review article on the formation, mechanism and biochemistry of MDA and MDA as a biomarker of oxidative stress. Int. J. Adv. Res. 2017; 5:811-8.
22. Khoubnasabjafari M, Ansarin K, Jouyban A. Reliability of malondialdehyde as a biomarker of oxidative stress in psychological disorders. BioImpacts: BI. 2015 Jul 26;5(3):123.
23. Takhtfooladi MA, Shahzamani M, Asghari A, Fakouri A. Naloxone pretreatment prevents kidney injury after liver ischemia reperfusion injury. International urology and nephrology. 2016 Jul;48(7):1113-20.
24. Wang X, Sun ZJ, Wu JL, Quan WQ, Xiao WD, Chew H, Jiang CM, Li D. Naloxone attenuates ischemic brain injury in rats through suppressing the NIK/IKKα/NF-κB and neuronal apoptotic pathways. Acta Pharmacologica Sinica. 2019 Feb;40(2):170-9.
25. Lin HY, Chang YY, Kao MC, Huang CJ. Naloxone inhibits nod-like receptor protein 3 inflammasome. Journal of Surgical Research. 2017 Nov 1;219: 72-7.

Table 1: Mean level of serum Alanine aminotransferase (ALT) (u/L) in the studied groups (n=10):

Group	Mean ± SEM	p- value
C-group	28.79± 0.26	
SC-group	30.14± 0.28	0.3455[#]
LIR group	48.43 ± 0.64	<0.0001[#*] <0.0001[$*]
LIR+ naloxone group	40.90 ± 0.42	<0.0001[#*] <0.0001[$*] <0.0001[&*]

[#] versus C-group, [$] versus SC-group, [&] versus LIR group, *p <0.05 is significant.

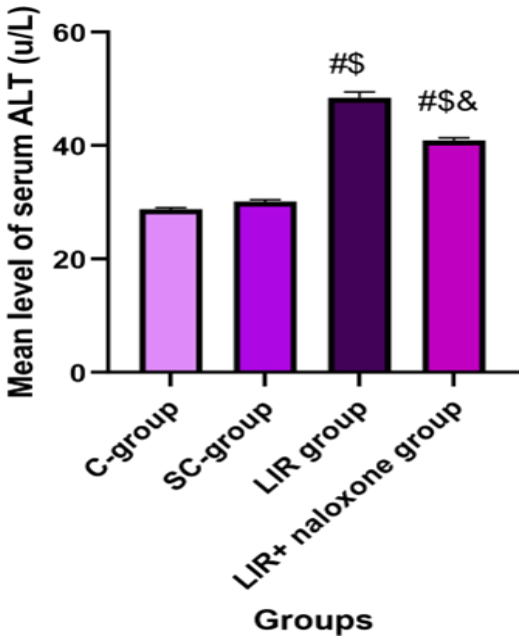

Histogram 1: Mean level of serum alanine aminotransferase (ALT) (u/L) in the studied groups (n=10), # versus C-group, $ versus SC-group, & versus LIR group, *p <0.05 is significant.

Table 2: Mean level of serum AST (aspartate aminotransferase) (u\L) in the studied groups (n=10):

Group	Mean ± SEM	p- value
C-group	94.88± 0.79	
SC-group	117.3± 1.05	0.0013$^{\#*}$
LIR group	264.6 ± 6.48	<0.0001$^{\#*}$ <0.0001$^{\$*}$
LIR+ naloxone group	210.5 ± 3.64	<0.0001$^{\#*}$ <0.0001$^{\$*}$ <0.0001$^{\&*}$

$^{\#}$ versus C-group, $^{\$}$ versus SC-group, $^{\&}$ versus LIR group, *p <0.05 is significant.

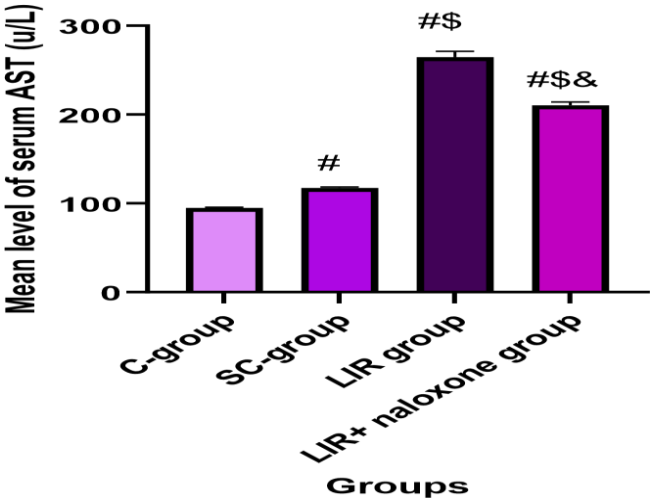

Histogram2: Mean level of serum aspartate aminotransferase (AST) (u/L) in the studied groups (n=10), # versus C-group, $ versus SC-group, & versus LIR group, *p <0.05 is significant.

Table 3 Mean level of serum urea (mg/dl) in the studied groups (n=10):

Group	Mean ± SEM	p- value
C-group	22.69 ± 0.23	
SC-group	33.41± 0.59	<0.0001$^{\#*}$
LIR group	43.34 ± 0.49	<0.0001$^{\#*}$ <0.0001$^{\$*}$
LIR+ naloxone group	37.03 ± 0.53	<0.0001$^{\#*}$ <0.0001$^{\$*}$ <0.0001$^{\&*}$

$^{\#}$ versus C-group, $^{\$}$ versus SC-group, $^{\&}$ versus LIR group, *p <0.05 is significant.

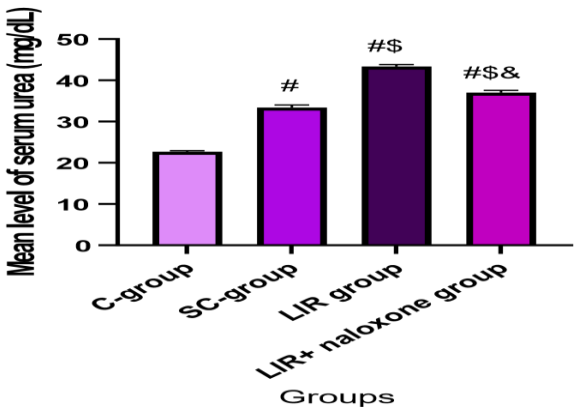

Histogram3: Mean level of serum urea (mg/dl) in the studied groups (n=10), # versus C-group, $ versus SC-group, & versus LIR group, *p <0.05 is significant.

Table 4: Mean level of serum creatinine (mg/dl) in the studied groups (n=10):

Group	Mean ± SEM	p- value
C-group	0.61± 0.03	
SC-group	0.76 ± 0.02	0.5316$^{\#}$
LIR group	2.9 ± 0.15	<0.0001$^{\#*}$ <0.0001$^{\$*}$
LIR+ naloxone group	1.49 ± 0.03	<0.0001$^{\#*}$ <0.0001$^{\$*}$ <0.0001$^{\&*}$

$^{S\#}$ versus C-group, $^{\$}$ versus SC-group, $^{\&}$ versus LIR group, *p <0.05 is significant.

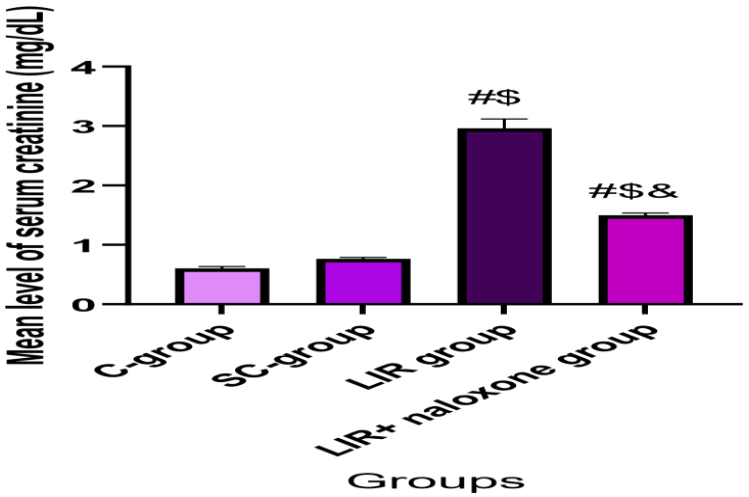

Histogram 4: Mean level of serum creatinine (mg/dl) in the studied groups (n=10),
versus C-group, $ versus SC-group, & versus LIR group, *p <0.05 is significant.

Table 5 Mean level of malondialdehyde (MDA) in renal tissue (nmol\ml) in the studied groups (n=10):

Group	**Mean ± SEM**	**p- value**
C-group	193.6 ± 0.98	
SC-group	196.8 ± 2.9	0.8171$^{\#}$
LIR group	400.1 ± 3.65	<0.0001$^{\#*}$ <0.0001$^{\$*}$
LIR+ naloxone group	247 ± 2.23	<0.0001$^{\#*}$ <0.0001$^{\$*}$ <0.0001$^{\&*}$

$^{\#}$ versus C-group, $^{\$}$ versus SC-group, $^{\&}$ versus LIR group, *p <0.05 is significant.

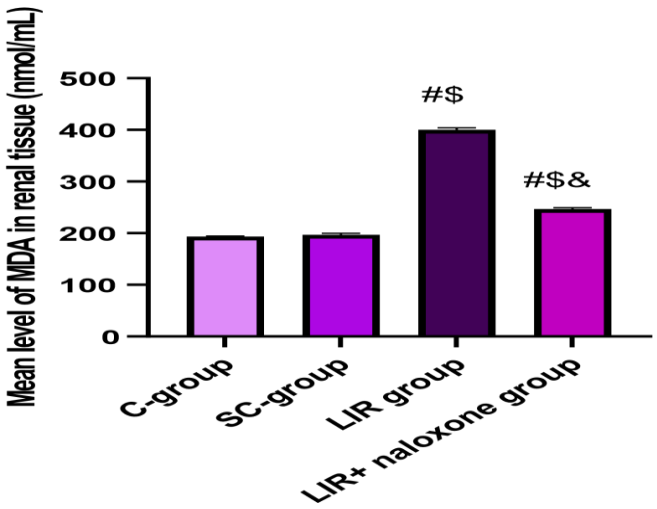

Groups
Histogram 5: Mean level of malondialdehyde (MDA) in renal tissue (nmol\ml) in the studied groups (n=10), # versus C-group, $ versus SC-group, & versus LIR group, *p <0.05 is significant.

Table 6 Mean level of tumor necrosis factor (TNF-α) in renal tissue (pg/mg) in the studied groups (n=10):

Group	Mean ± SEM	p- value
C-group	84.6 ± 2.07	
SC-group	90.64 ± 1.26	0.048#*
LIR group	134.7 ± 1.68	<0.0001#* <0.0001$*
LIR+ naloxone group	105.7 ± 0.96	<0.0001#* <0.0001$* <0.0001&*

versus C-group, $ versus SC-group, & versus LIR group, *p <0.05 is significant.

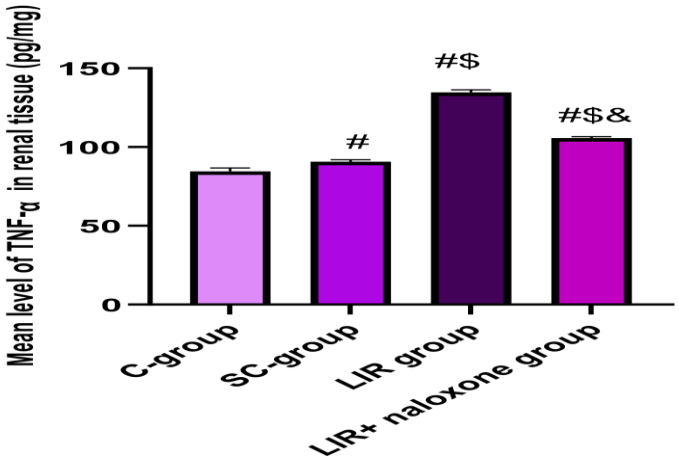

Histogram 6: Mean level of tumor necrosis factor (TNF-α) in renal tissue (pg/mg) in the studied groups (n=10), # versus C-group, $ versus SC-group, & versus LIR group, *p <0.05 is significant.

Table 7 Mean surface area fraction of COX-2 immunoreactivity in kidney tissue in the studied groups (n=10):

Group	Mean ± SEM	p- value
C-group	1.061 ± 0.035	
SC-group	1.113 ± 0.047	0.999#
LIR group	40.76 ± 1.01	<0.0001#* <0.0001$*
LIR+ naloxone group	25.04 ± 1.52	<0.0001#* <0.0001$* <0.0001&*

versus C-group, $ versus SC-group, & versus LIR group, *p <0.05 is significant.

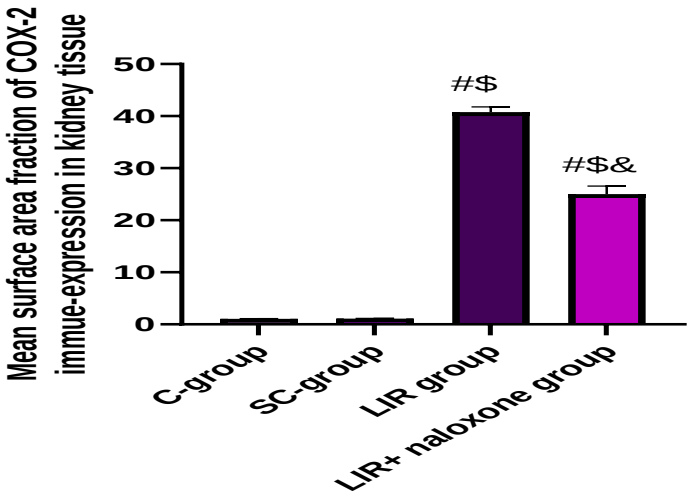

Histogram 7: Mean surface area fraction of COX-2 immunoreactivity in kidney tissue in the studied groups (n=10), # versus C-group, $ versus SC-group, & versus LIR group, *p <0.05 is significant.

Table 8 Mean surface area fraction of NF-κB immunoreactivity in kidney tissue in the studied groups (n=10):

Group	Mean ± SEM	p- value
C-group	1.133 ± 0.13	
SC-group	1.20 ± 0.11	0.999[#]
LIR group	34.13 ± 0.89	<0.0001[#*] <0.0001[$*]
LIR+ naloxone group	18.46 ± 0.93	0.0001[#*] 0.0001[$*] <0.0001[&*]

[#] versus C-group, [$] versus SC-group, [&] versus LIR group, *p <0.05 is significant.

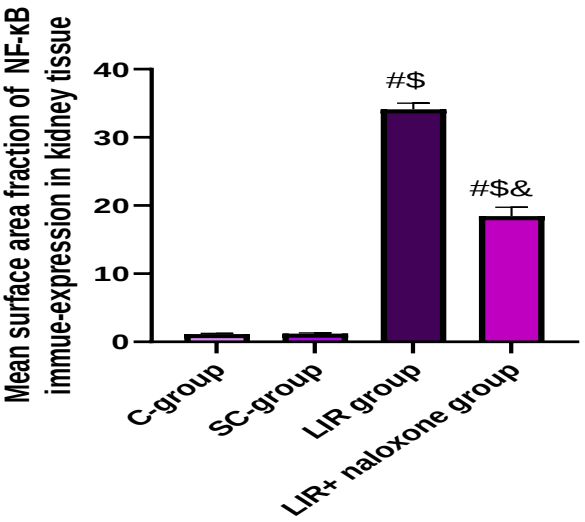

Histogram 8: Mean surface area fraction of NF-κB immunoreactivity in kidney tissue in the studied groups (n=10), [#] versus C-group, [$] versus SC-group, [&] versus LIR group, *p <0.05 is significant.

Table 9 Mean surface area fraction of caspase-3 immunoreactivity in kidney tissue in the studied groups (n=10):

Group	Mean ± SEM	p- value
C-group	1.14 ± 0.20	
SC-group	1.17 ± 0.13	0.999[#]
LIR group	32.21 ± 1.05	<0.0001[#*] <0.0001[$*]
LIR+ naloxone group	15.61 ± 0.36	<0.0001[#*] <0.0001[$*] <0.0001[&*]

[#] versus C-group, [$] versus SC-group, [&] versus LIR group, *p <0.05 is significant.

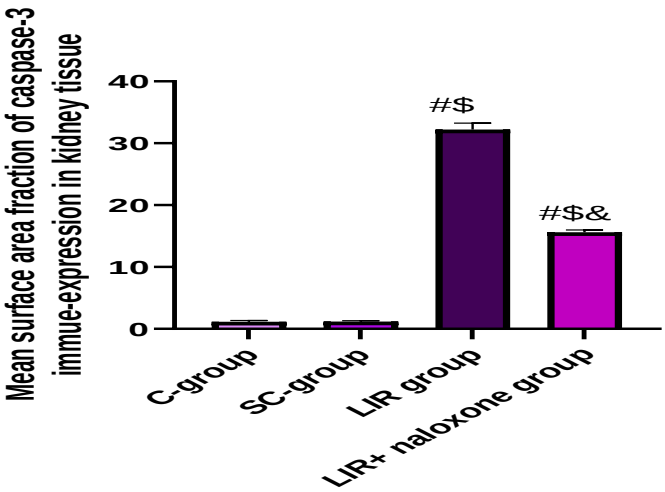

Histogram 9: Mean surface area fraction of caspase-3 immunoreactivity in kidney tissue in the studied groups (n=10), [#] versus C-group, [$] versus SC-group, [&] versus LIR group, *p <0.05 is significant.

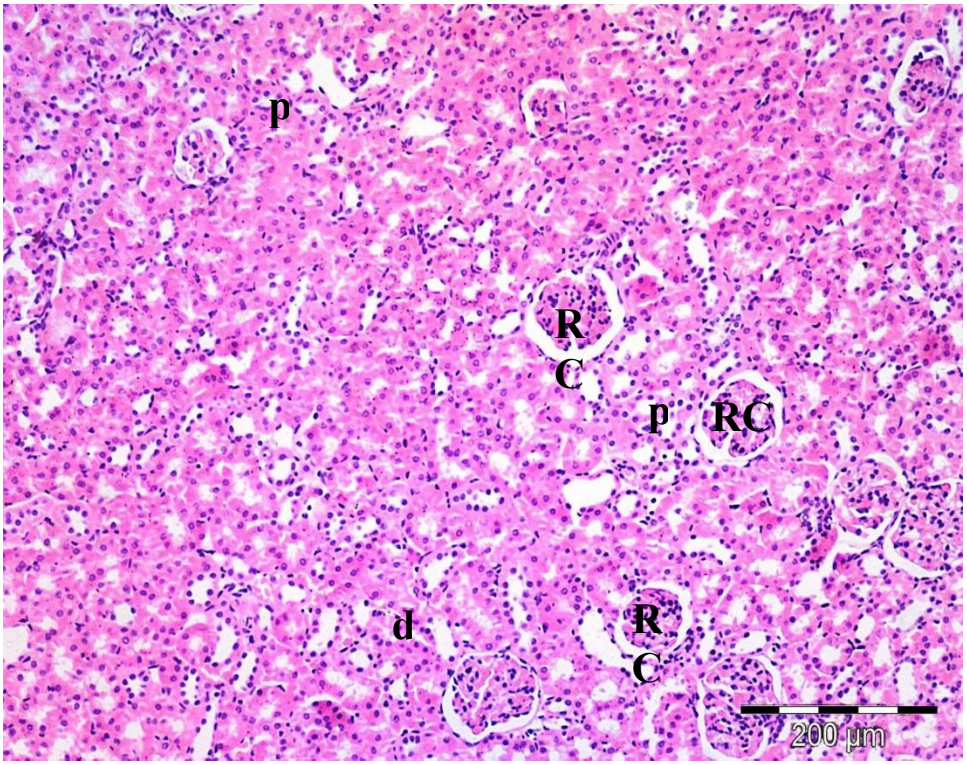

Fig.1: A photomicrograph of kidney tissue section of **C-group** showing normal organization of the renal cortex consisting of renal corpuscles (RC), PCTs (p) and DCTs (d).
H&E X100

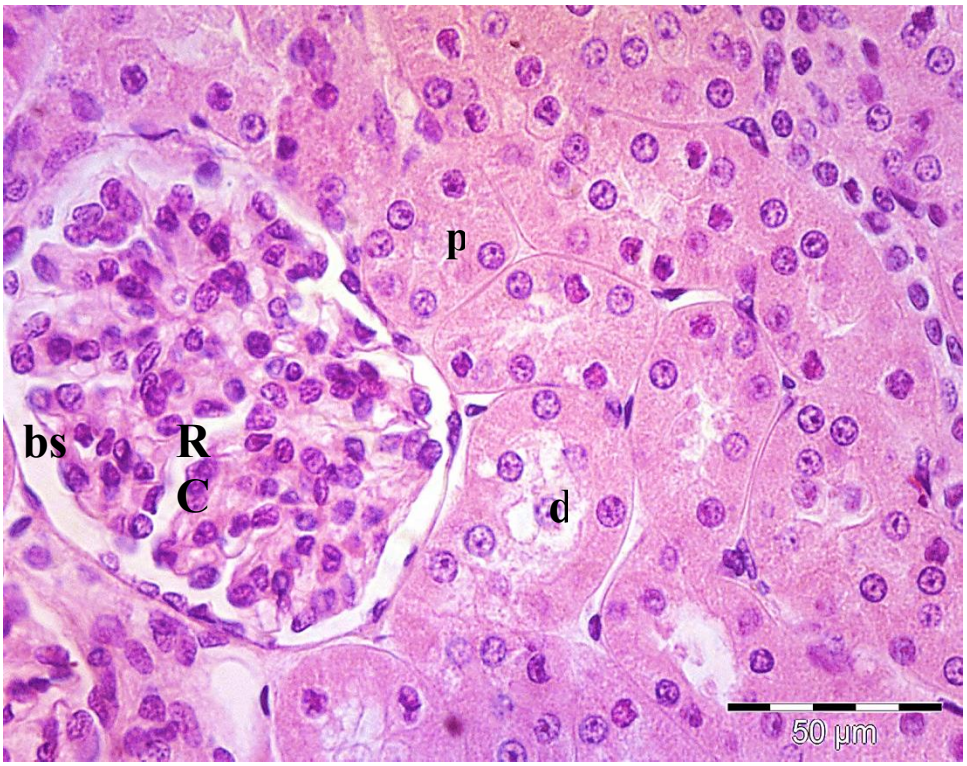

Fig. 2: A photomicrograph of kidney tissue section of **C-group** showing normal structure of renal corpuscles (RC), Bowman's space (bs), PCTs (p) and DCTs (d). PCTs lined with cuboidal cells of acidophilic cytoplasm with central rounded vesicular nuclei. DCTs with wider lumina lined with less acidophilic cuboidal cells.
H&E x400

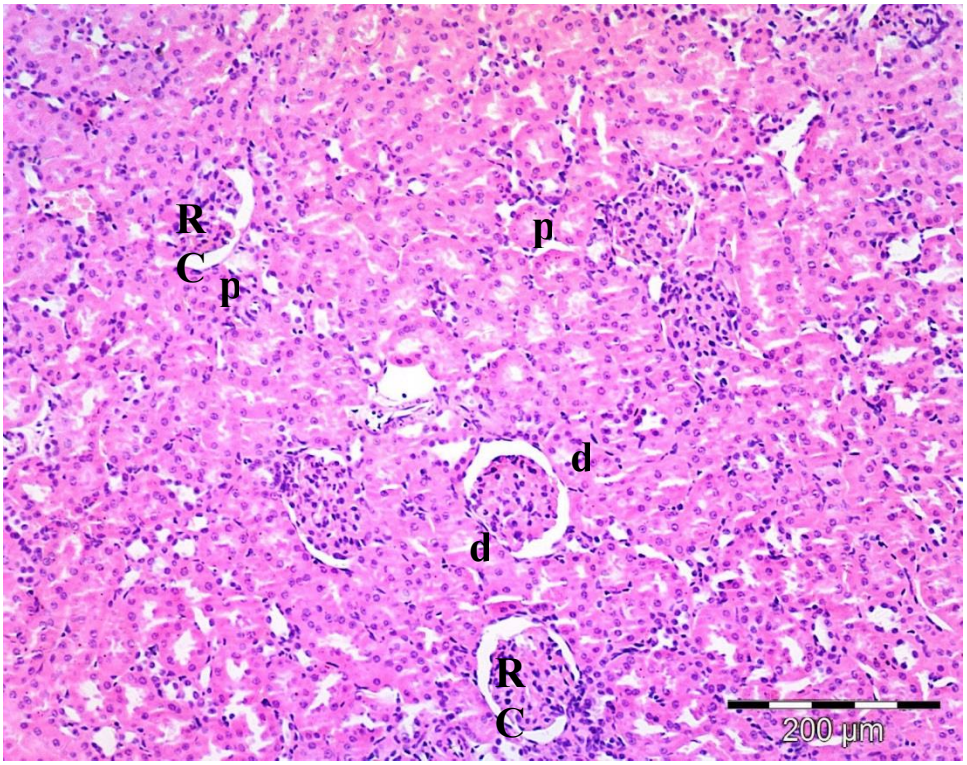

Fig.3: A photomicrograph of kidney tissue section of **SC-group** showing normal organization of the renal cortex consisting of renal corpuscles (RC), PCTs (p) and DCTs (d).
H&E X100

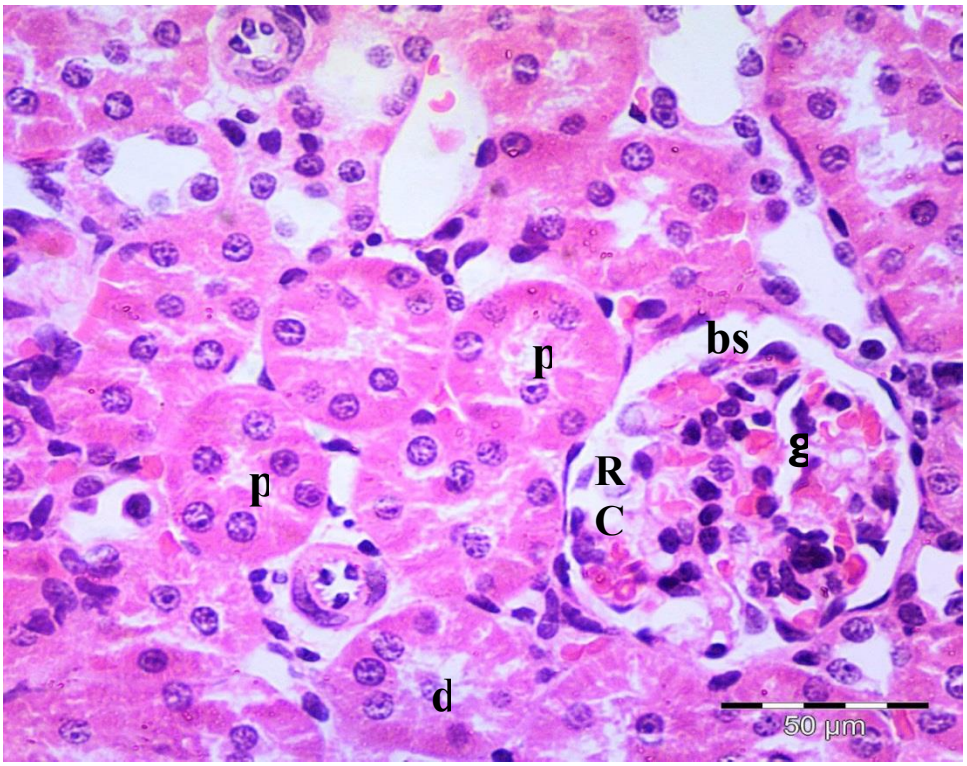

Fig.4: A photomicrograph of kidney tissue section of **SC-group** showing normal structure of renal corpuscles (RC) except for congested glomerular capillaries (g), Bowman's space (bs), PCTs (p) and DCTs (d). PCTs lined with cuboidal cells of acidophilic cytoplasm with central rounded vesicular nuclei. DCTs with wider lumina lined with less acidophilic cuboidal cells.
H&E x400

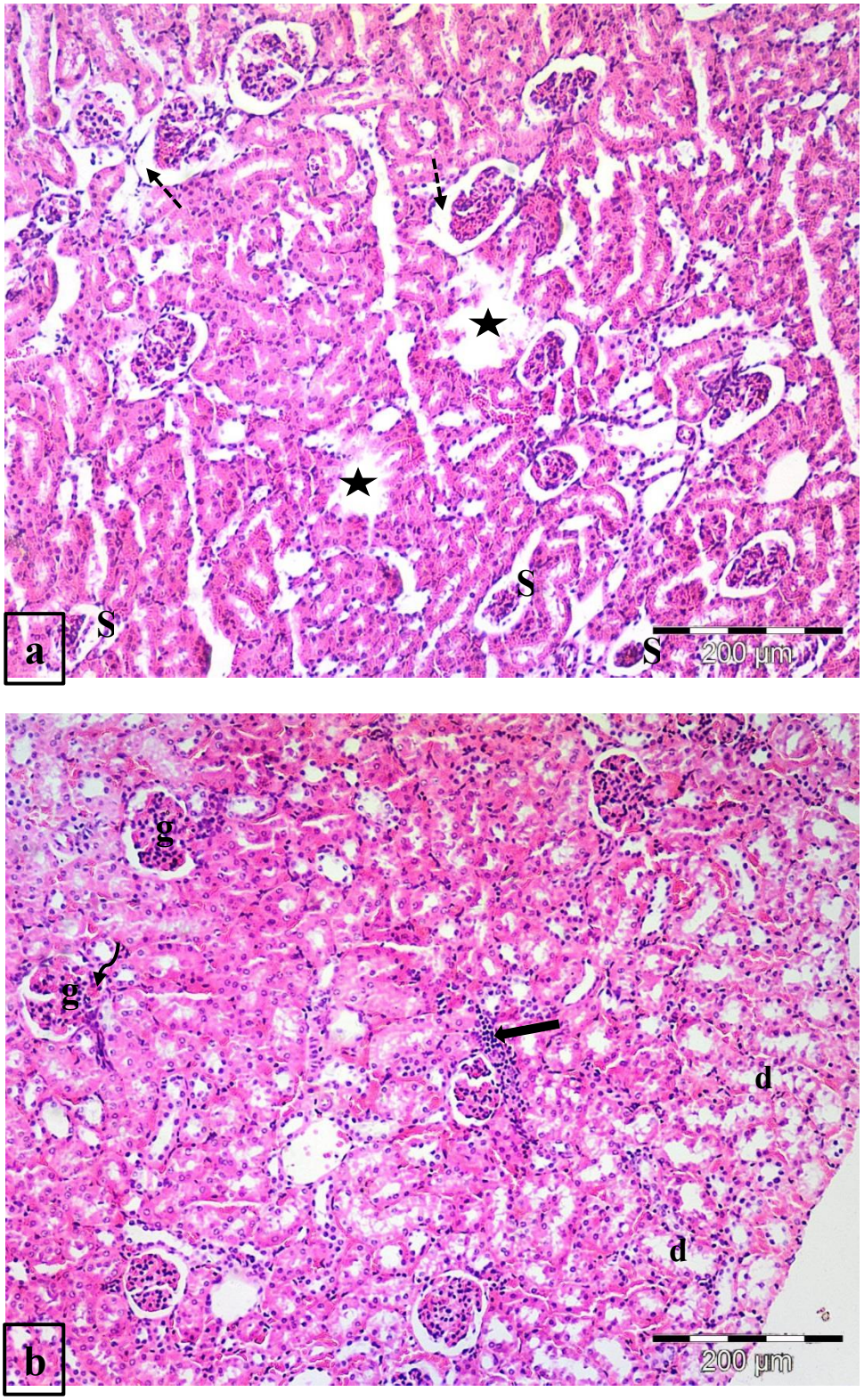

Fig. 5: photomicrographs of kidney tissue sections of **LIR group** showing:

a) Disruption of normal organization of the renal cortex with areas of focal loss (stars), shrunken distorted renal corpuscles (S) with widening of bowman's space (dotted arrow).

b) Other areas showed hypertrophied renal corpuscle (g) with narrowing of bowman's space (curved arrow). Notice dilatation of some tubular lumina (d) and inflammatory cellular infiltrate (thick arrow).

H&E X100

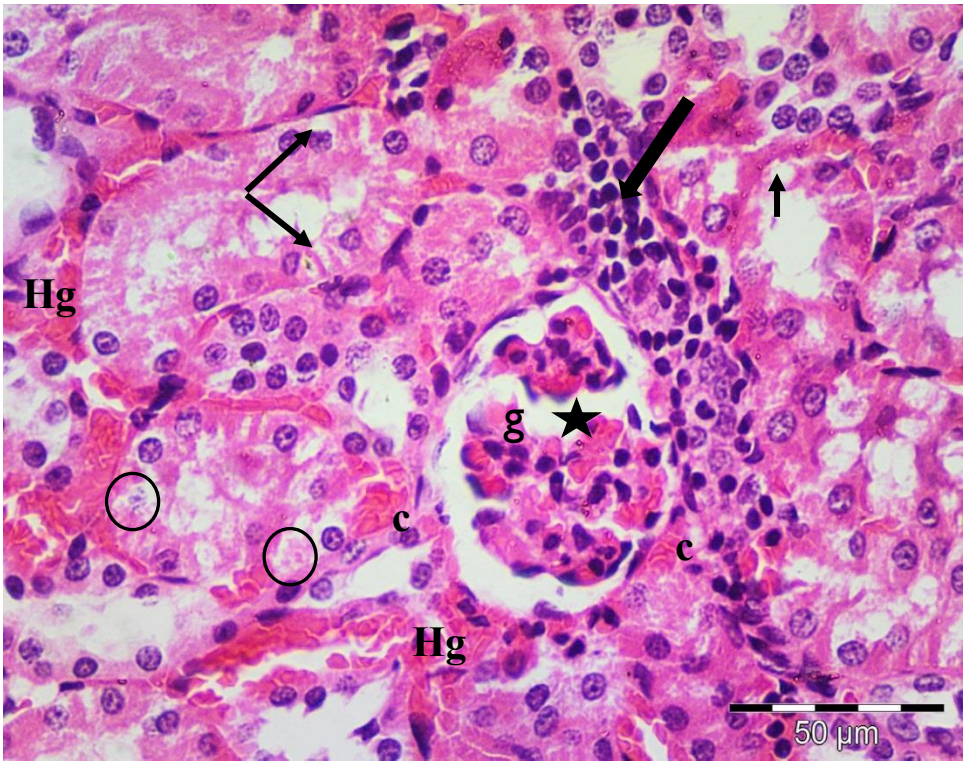

Fig.6: A photomicrograph of kidney tissue section of **LIR group** showing distorted renal corpuscle (star), congested glomerular capillaries (g), congestion of peritubular capillaries (c) and interstitial hemorrhage (Hg). Tubular distortion; vacuolation of some tubular cells (thin arrows), and other cells with ghosts of the nuclei and disappearance of cytoplasm (circles). Notice inflammatory cell infiltrate mostly lymphocytes (thick arrow).
H&E X400

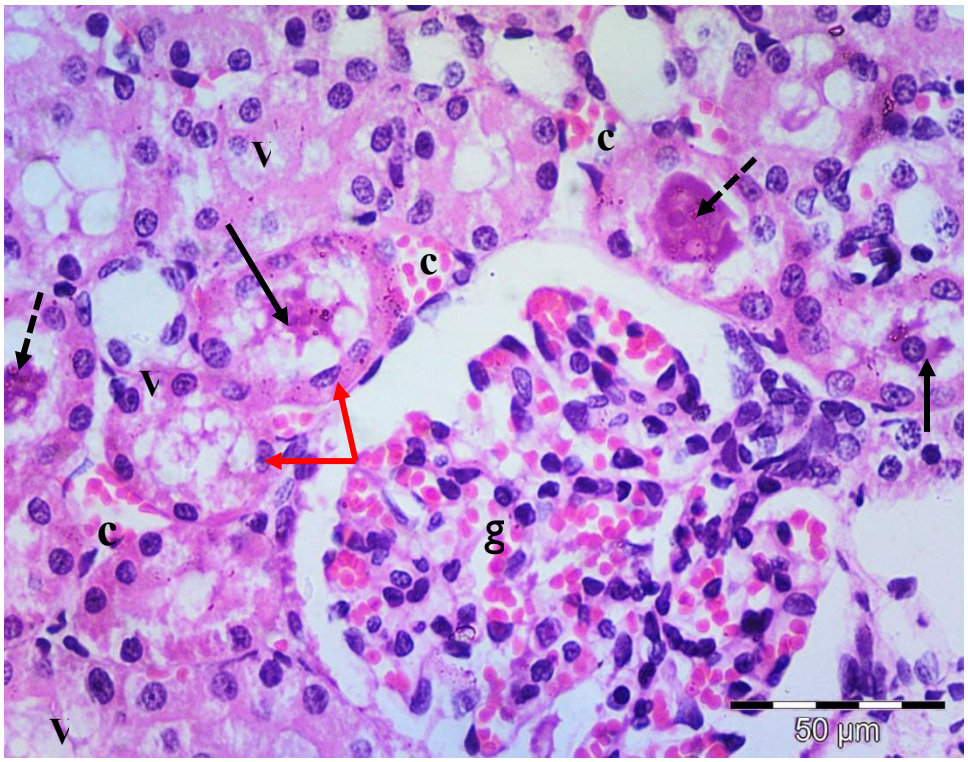

Fig.7: A photomicrograph of kidney tissue section of **LIR group** showing congested glomerular capillaries (g), congestion of peritubular capillaries (c), vacuolation of some tubular cells (V), flattening of some epithelial lining (red arrows) with desquamation of some cells with cellular debris in tubular lumina (arrow). Notice some tubular lumina with eosinophilic material; hyaline casts (dotted arrows).
H&E X400

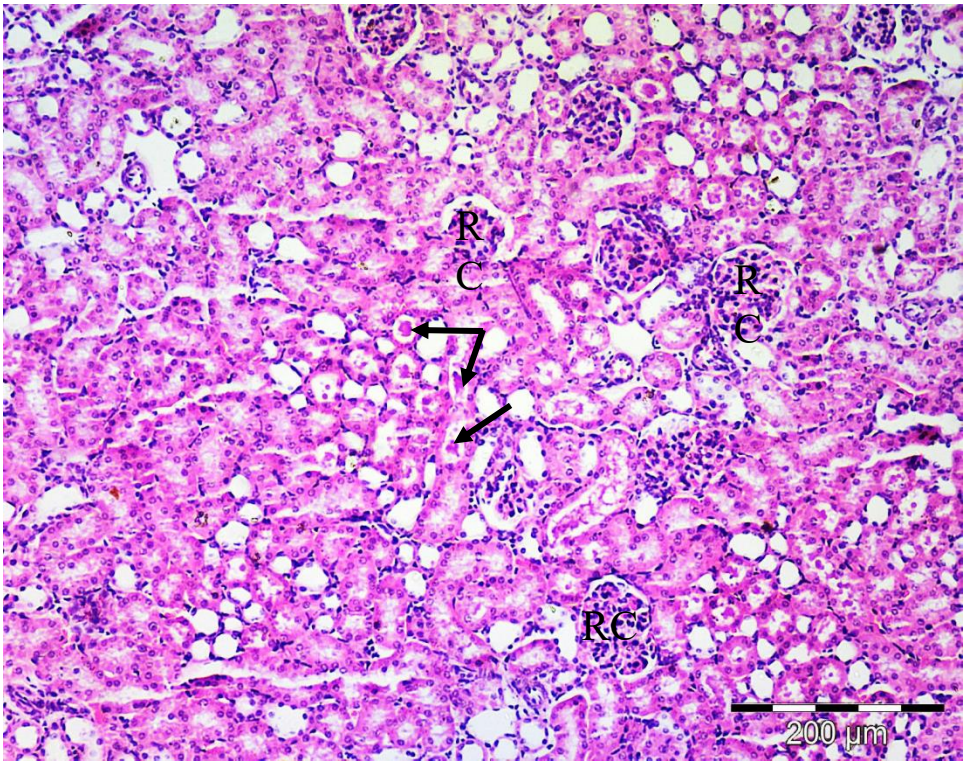

Fig.8: A photomicrograph of kidney tissue section of **LIR+ naloxone group** showing restoration of normal appearance of renal cortex; renal corpuscles (RC) and tubules. Notice some hyaline casts in some tubular lumina (arrows).
H & E × 100

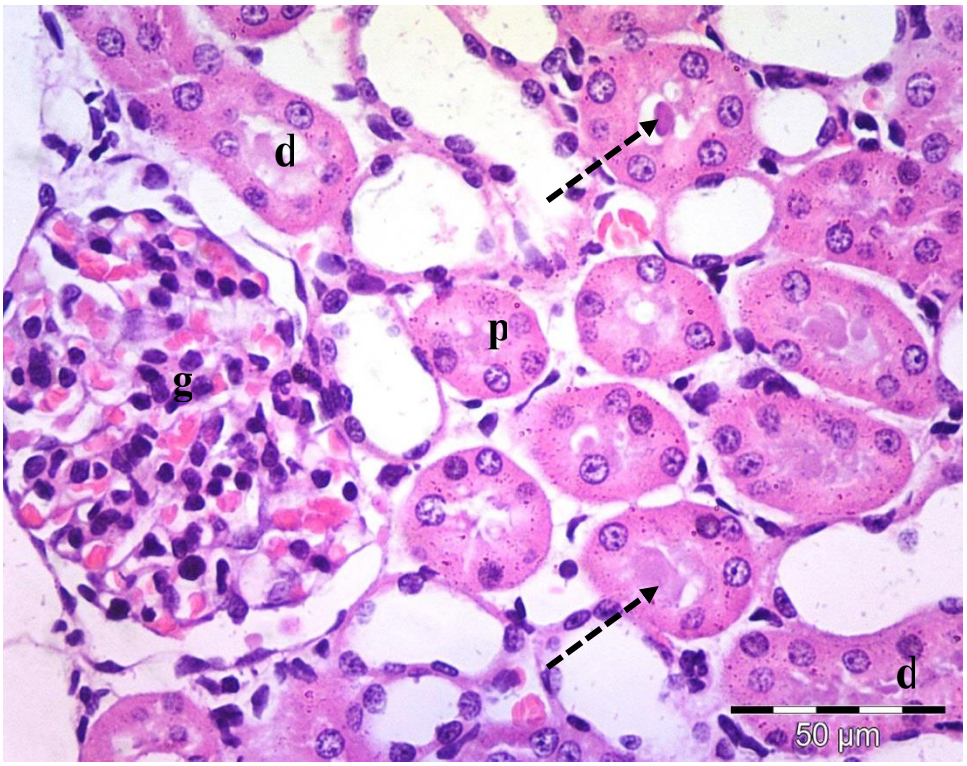

Fig. 9: A photomicrograph of kidney tissue section of **LIR+ naloxone group** showing mild congestion of glomerular capillaries (g) and apparent normal PCTs (p) and DCTs (d)**.** Notice hyaline casts in some tubular lumina (dotted arrow).
H & E × 400

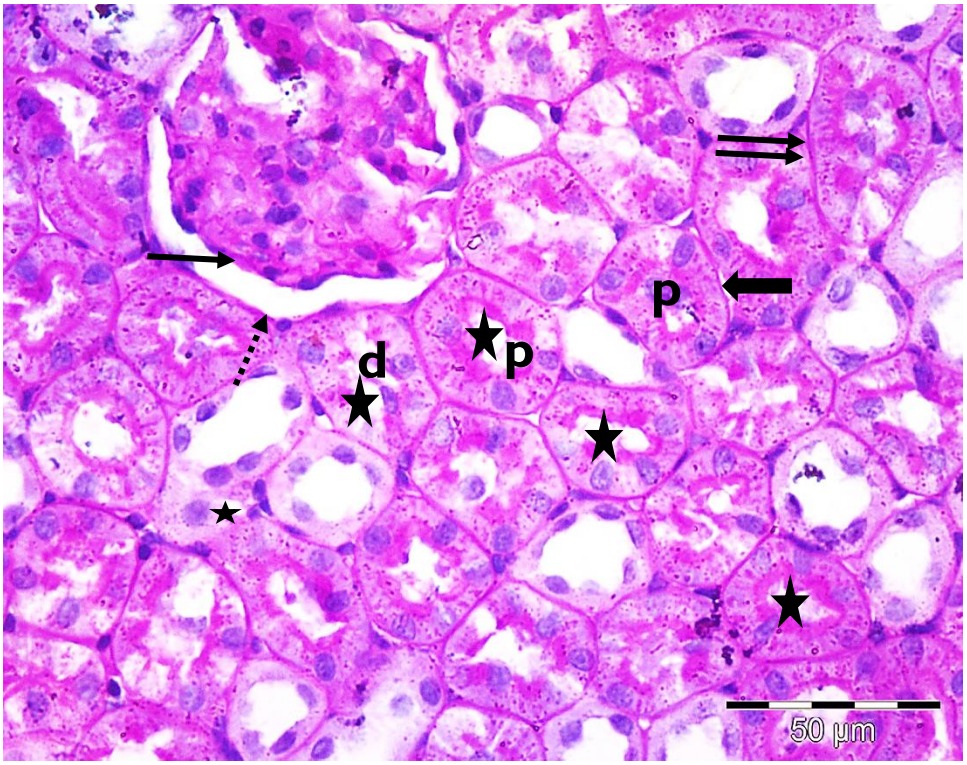

Fig.10: A photomicrograph of kidney tissue section of **C-group** showing positive PAS reaction in the BMs of glomerular blood capillaries (thin arrow), parietal layers of Bowman's capsules (dotted arrow), PCTs (thick arrows) and DCTs (double arrows) cells. Notice the staining of brush borders (stars) of the PCT (p) and DCT (d).
PAS X 400

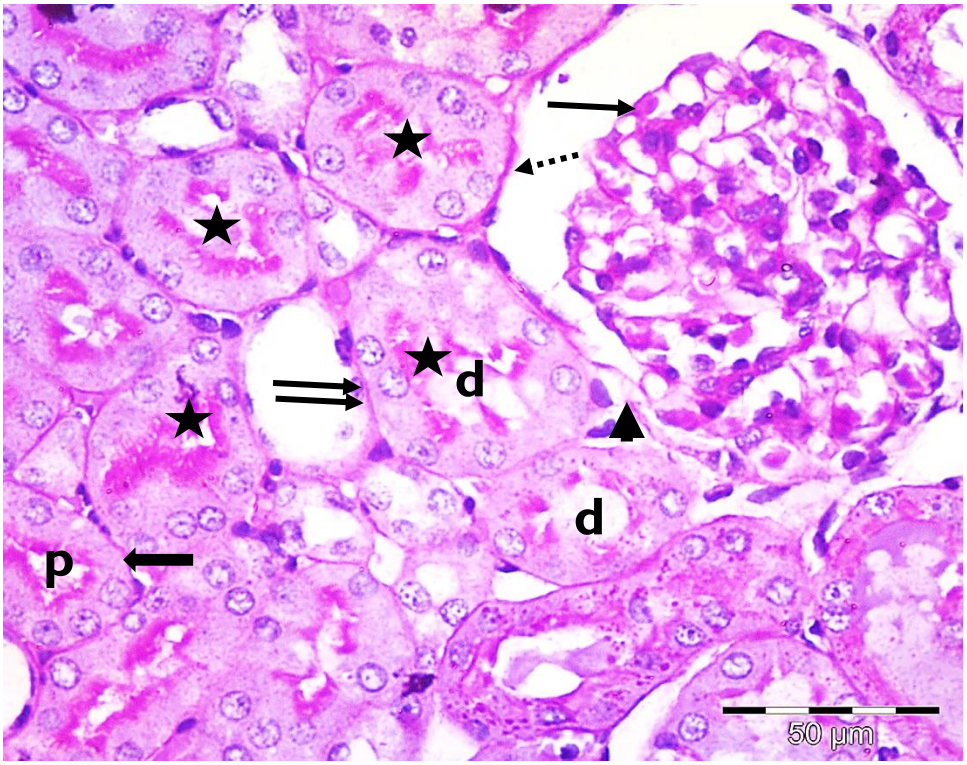

Fig.11: A photomicrograph of kidney tissue section of S**C-group** showing positive PAS reaction in the BMs of glomerular blood capillaries (thin arrow), parietal layers of Bowman's capsules (dotted arrow), PCTs (thick arrows) and DCTs (double arrows) cells. Notice the staining of brush borders (stars) of the PCT (p) and DCT (d) except for some areas of interruption of basement membrane of glomerular blood capillaries (arrow heads).
PAS X 400

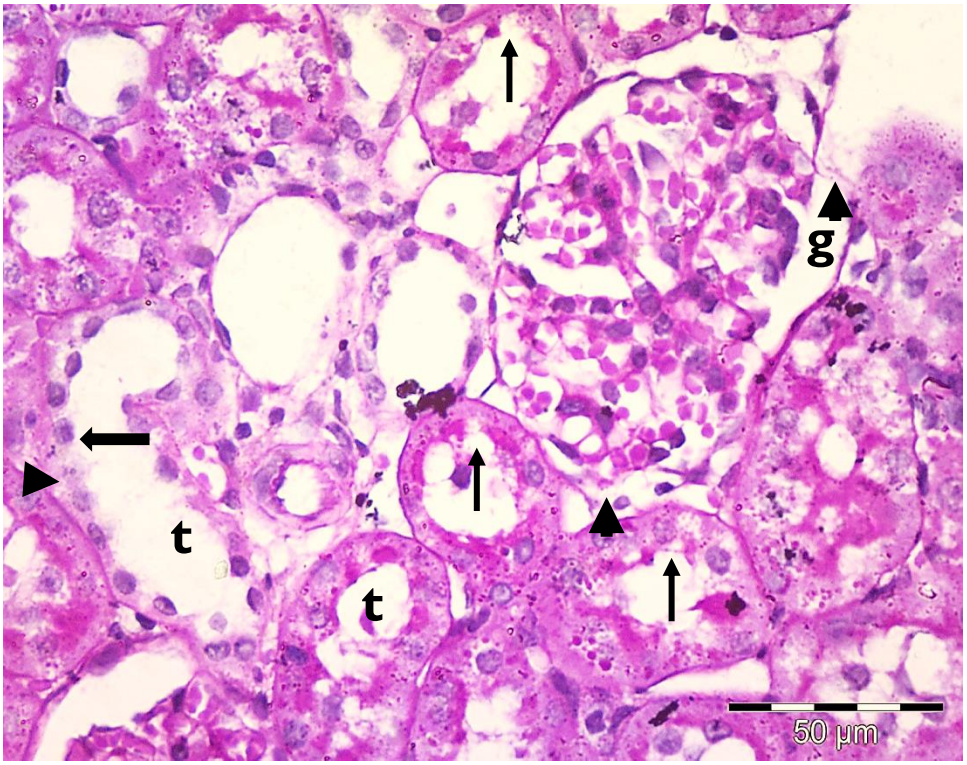

Fig.12: A photomicrograph of renal cortex of **LIR group** showing partial (thin arrows) or complete loss (thick arrows) of the brush border of distorted renal tubules. Notice interruption of basement membrane (arrow heads) of the distorted glomerulus (g) and tubules (t).
PAS X 400

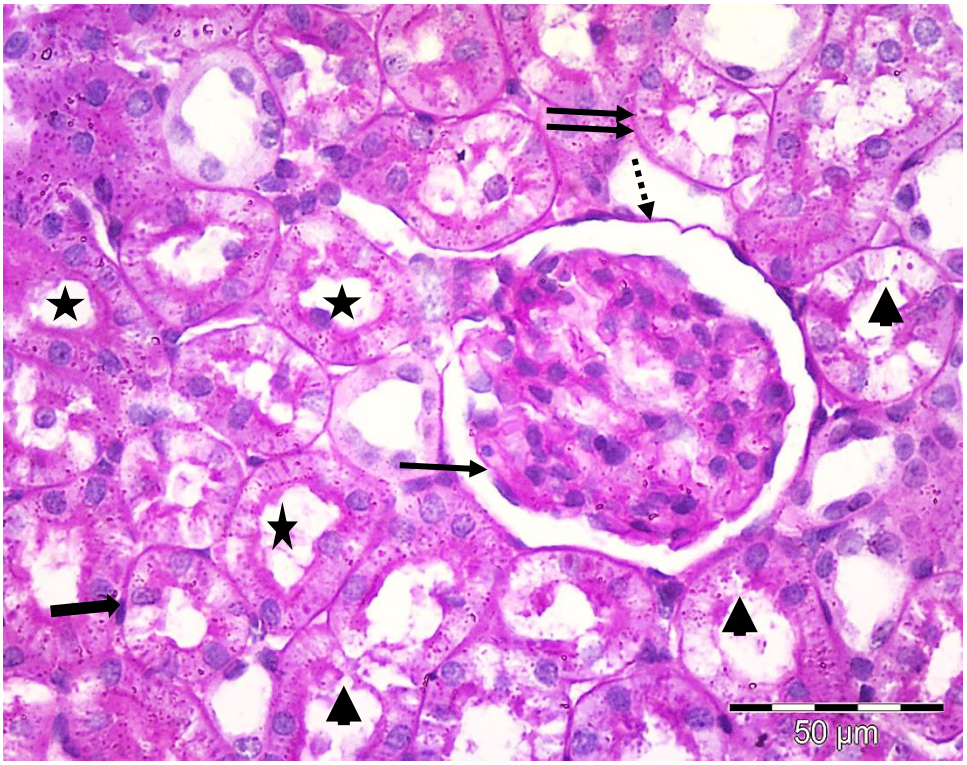

Fig.13: A photomicrograph of renal cortex of **LIR+ naloxone group** showing preserved reaction of most brush borders (stars) of PCTs (p), DCTs (d), continuous basement membranes of glomerular blood capillaries (thin arrow), parietal layers of Bowman's capsule (dotted arrow), PCTs (thick arrows) and DCTs (double arrows) cells. Notice some tubules showing partial loss of the brush border (arrow heads).
PAS X 400

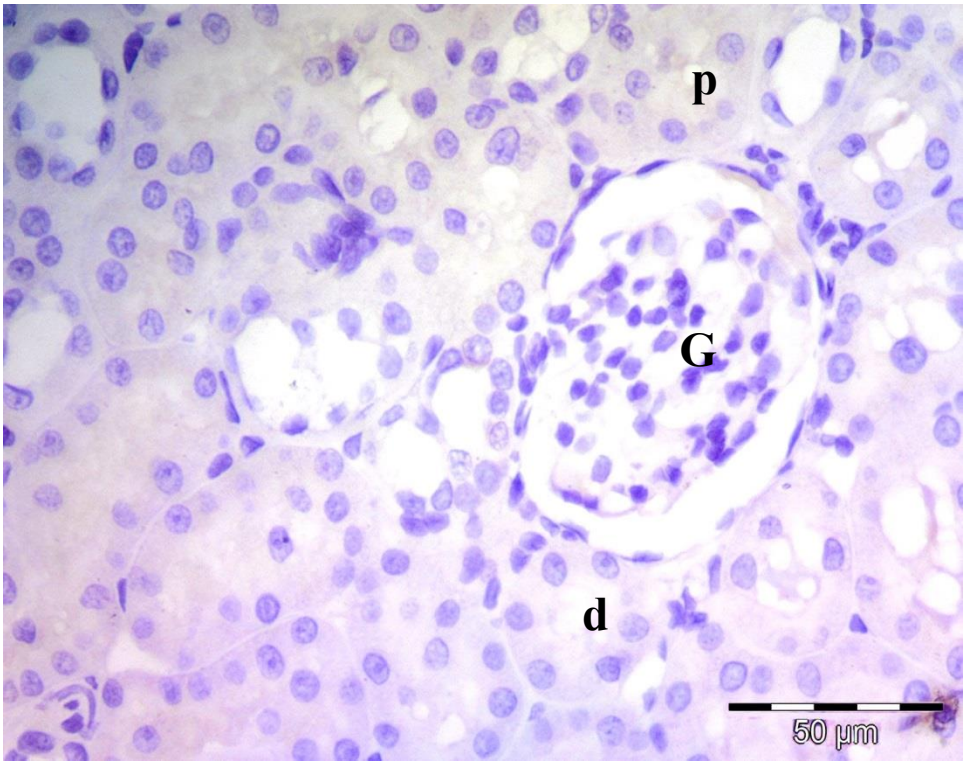

Fig.14: A photomicrograph of kidney of **C-group** showing negative COX-2 cytoplasmic immune expression in the glomerular (G), PCT (p) and DCT (d) cells.
COX-2 immunohistochemistry counterstained with H X 400

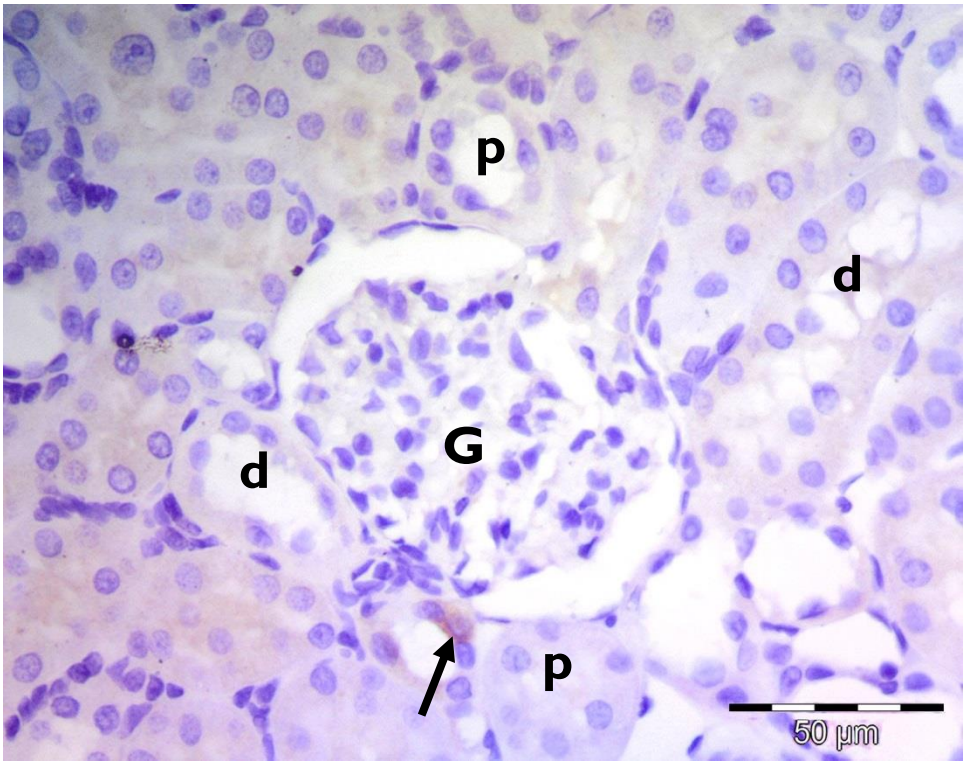

Fig.15: A photomicrograph of kidney of **SC-group** showing negative COX-2 cytoplasmic immune expression in the glomerular (G), PCT (p) and DCT (d) cells. Notice faint expression in few tubular cells (arrow)
Immunohistochemistry counterstained with H X 400

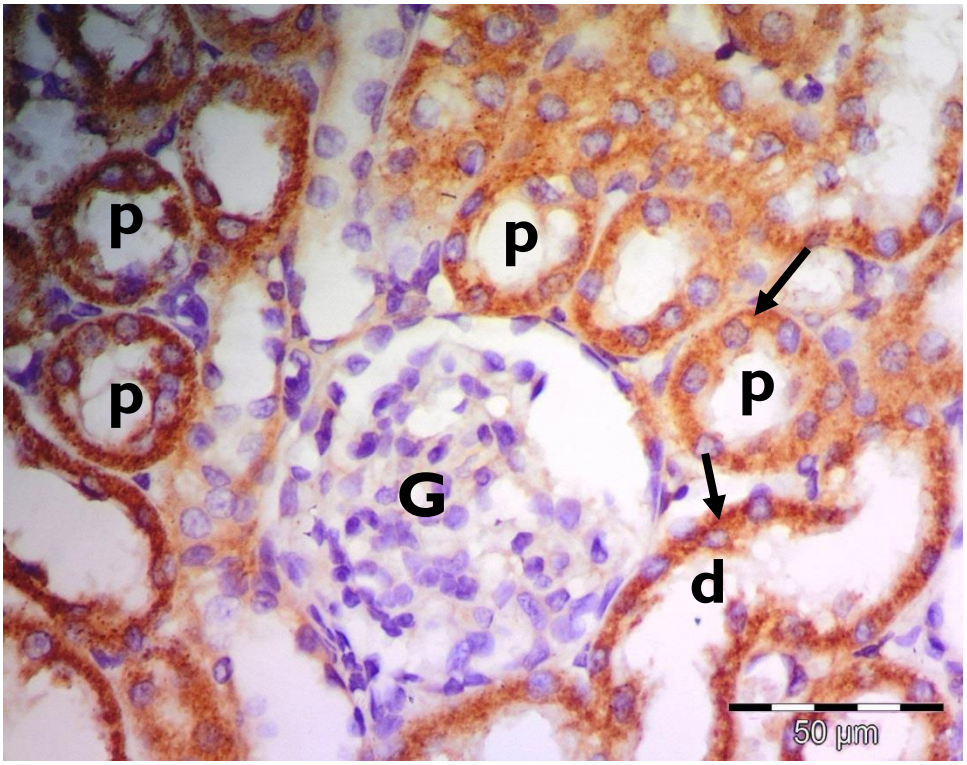

Fig. 16: A representative photomicrograph of a section in rat kidney of **LIR group** showing deeply stained cytoplasmic COX-2 immune reactivity in the tubular cells (arrows).
COX-2 Immunohistochemistry counterstained with H X 400

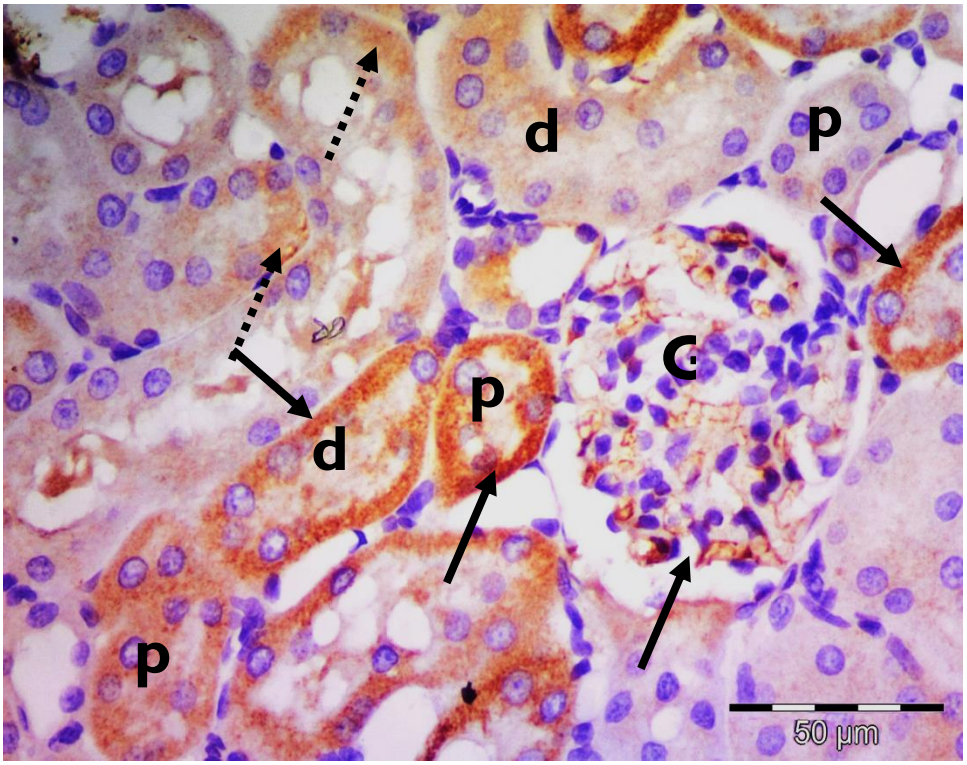

Fig.17: A representative photomicrograph of a section in rat kidney of **LIR group** showing deeply stained cytoplasmic COX-2 immune reactivity in the glomerular (G), PCT (p), DCT (d) cells (arrows) with some faint cytoplasmic reaction in other glomerular and tubular cells (dotted arrows).
COX-2 Immunohistochemistry counterstained with H X 400

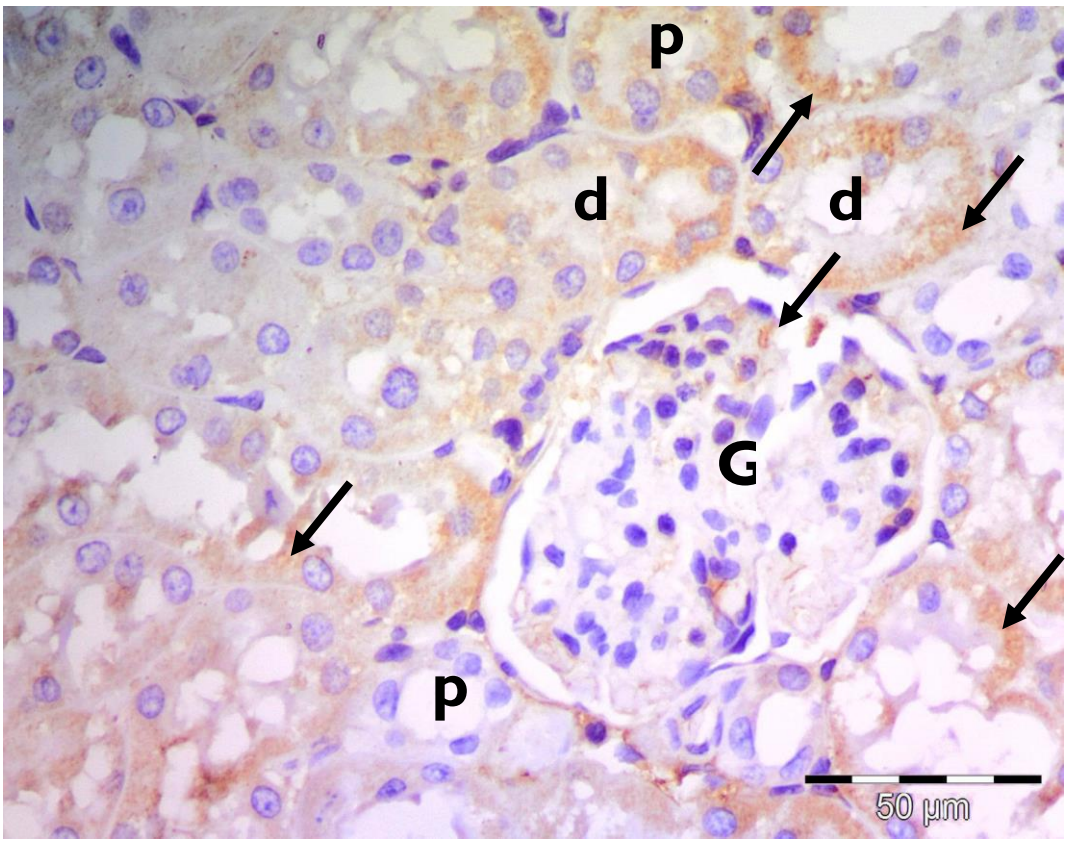

Fig.18: A representative photomicrograph of a section in rat kidney of **LIR+ naloxone group** showing faint COX-2 cytoplasmic expression (arrows) in most glomerular (G), PCT (p) , DCT (d) cells
COX-2 Immunohistochemistry counter stain H x400

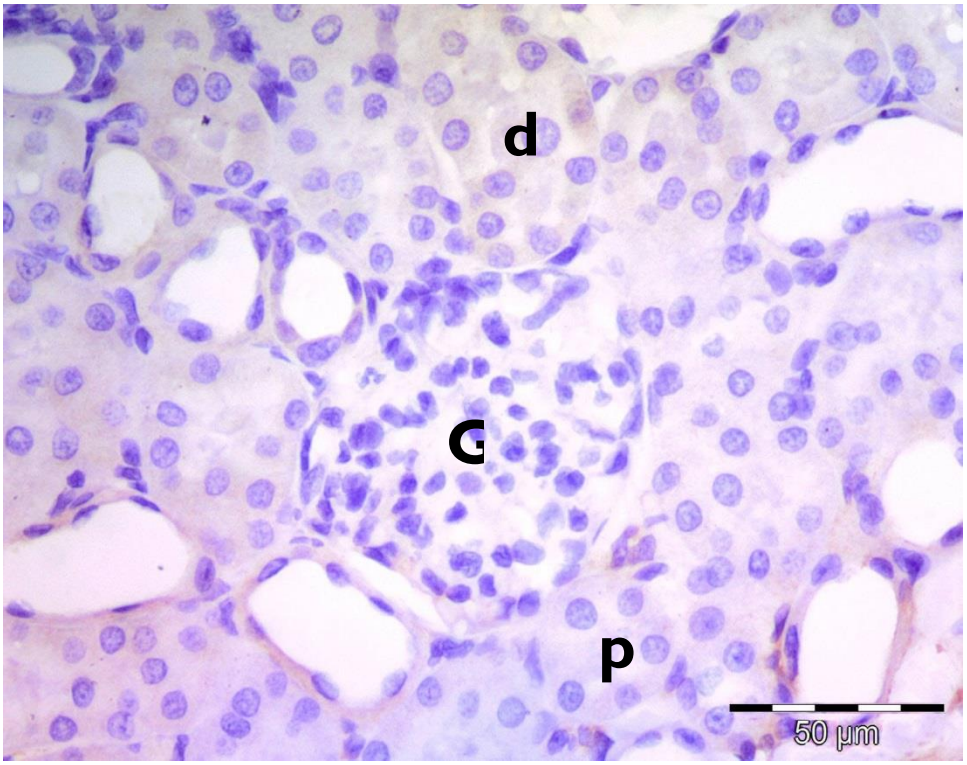

Fig. 19: A representative photomicrograph of a section in rat kidney of **C-group** showing negative NF-κB cytoplasmic immune expression in the glomerular (G), PCT (p) and DCT (d) cells.
NF-κB Immunohistochemistry counterstained with H X 400

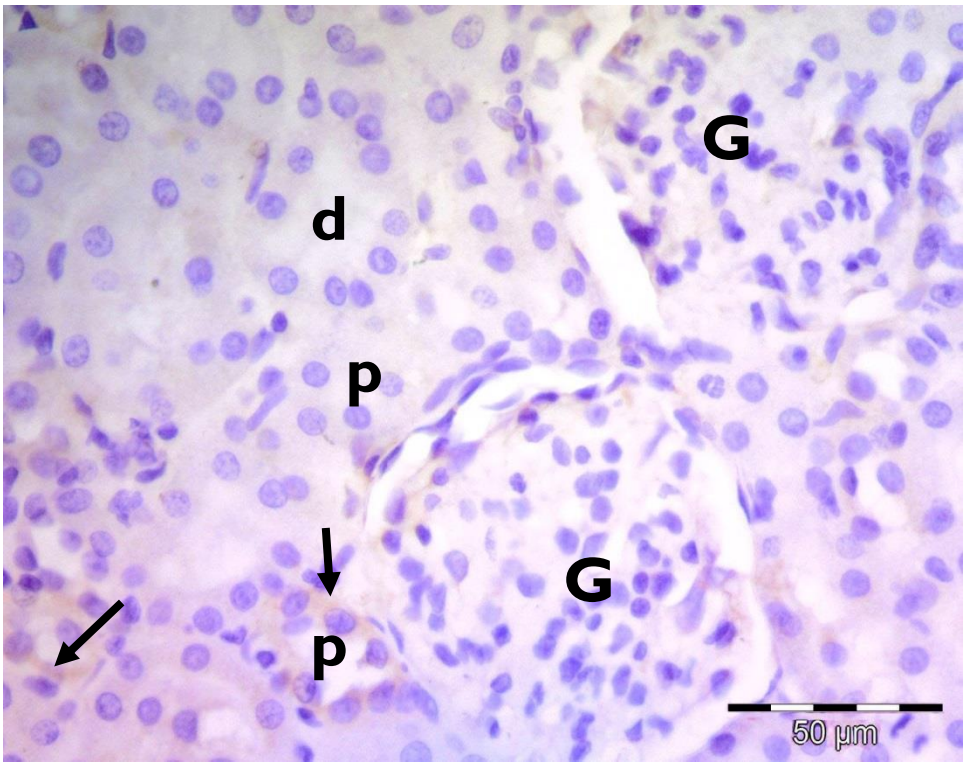

Fig. 20: A representative photomicrograph of a section in rat kidney of **SC-group** showing negative NF-κB cytoplasmic immune expression in the glomerular (G), PCT (p) and DCT (d) cells. Notice faint expression in few tubular cells (arrows).
NF-κB Immunohistochemistry counterstained with H X 400

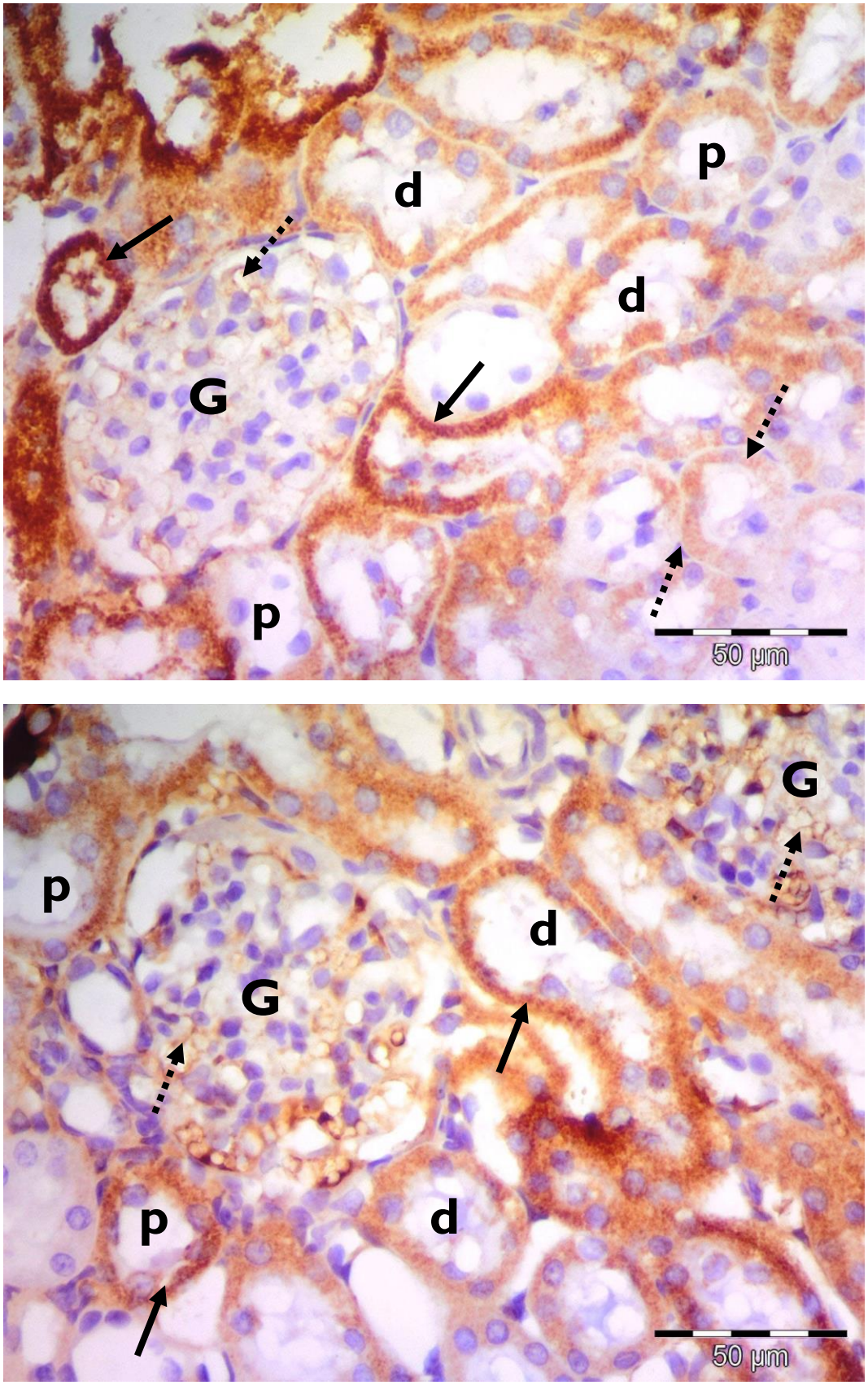

Fig.21: Representative photomicrographs of a section in rat kidney of **LIR group** showing deeply stained cytoplasmic NF-κB immune reactivity in PCT (p) and DCT (d) cells (arrows) with some faint cytoplasmic reaction in other glomerular and tubular cells (dotted arrows).
NF-κB Immunohistochemistry counterstained with H X 400

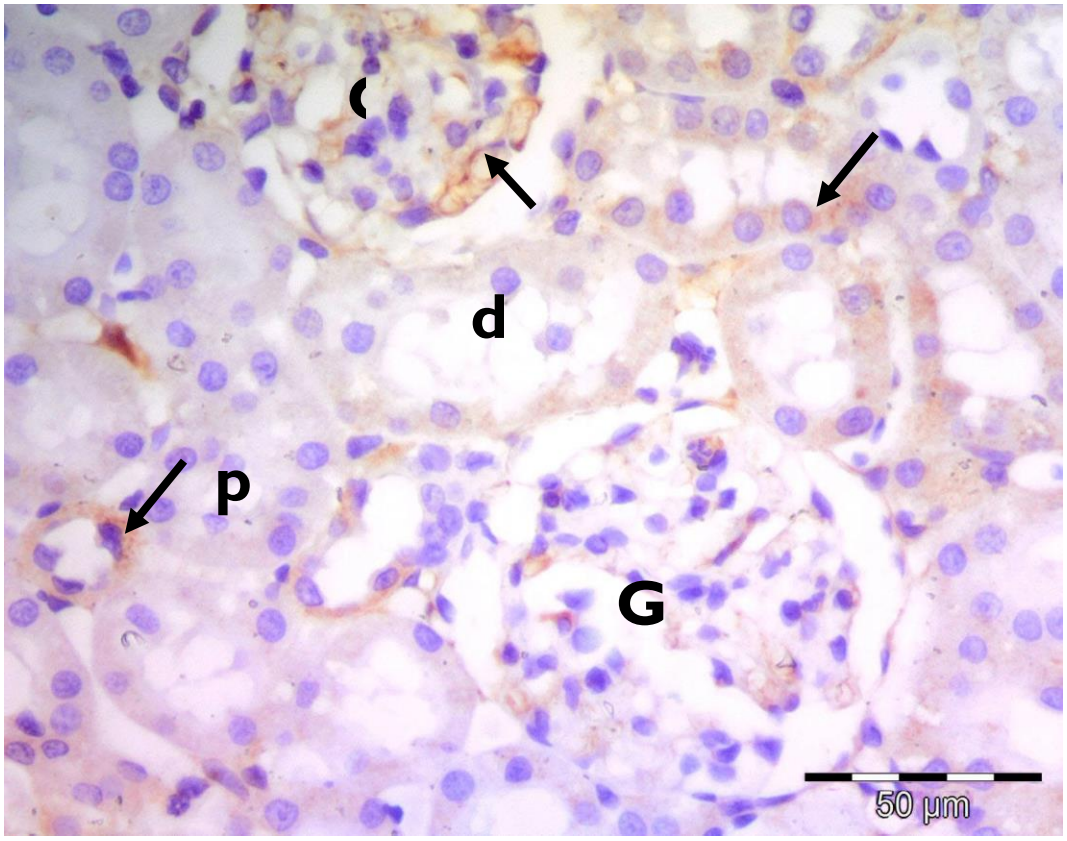

Fig.22: A representative photomicrograph of a section in rat kidney of **LIR+ naloxone group** showing faint NF-κB cytoplasmic expression (arrows) in some glomerular (G), PCT (p) , DCT (d) cells
NF-κB Immunohistochemistry counter stain H x400

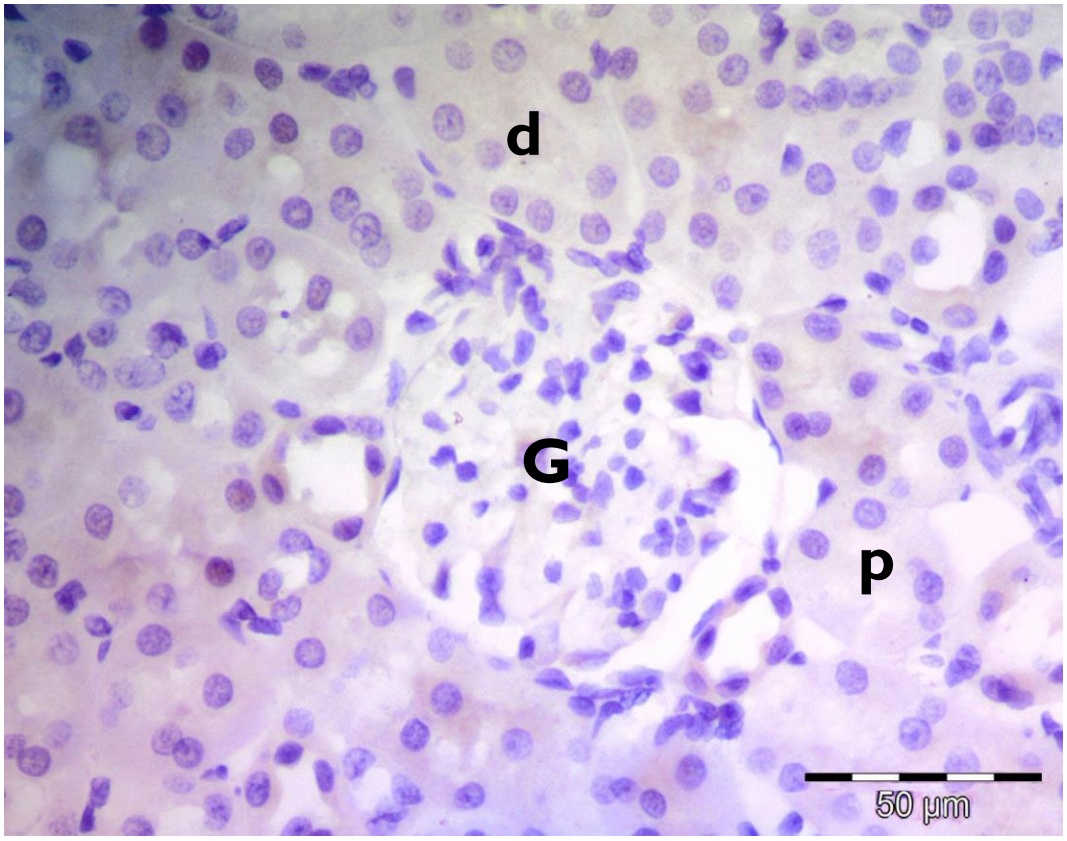

Fig.23: A representative photomicrograph of a section in rat kidney of **C-group** showing negative caspase-3 immune expression in the glomerular (G), PCT (p) and DCT (d) cells.
Caspase-3 Immunohistochemistry counterstained with H X 400

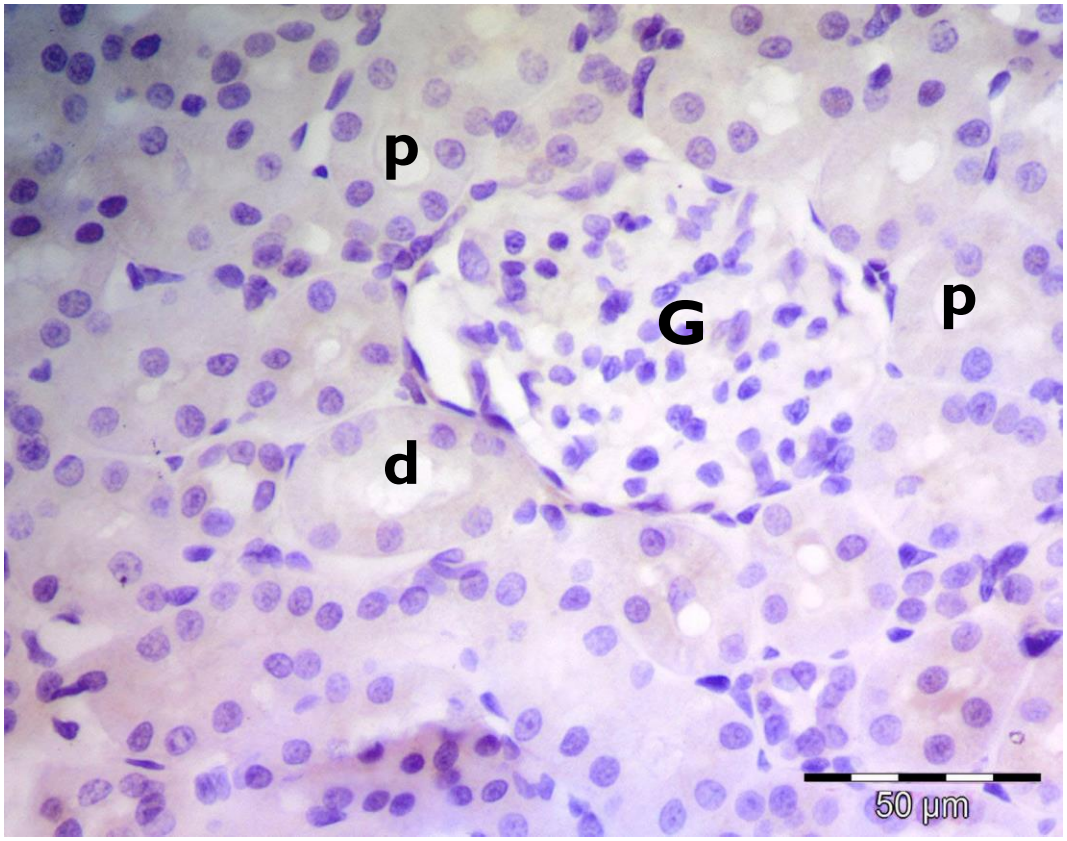

Fig.24: A representative photomicrograph of a section in rat kidney of **SC-group** showing negative caspase-3 immune expression in the glomerular (G), PCT (p) and DCT (d) cells.
Caspase-3 Immunohistochemistry counterstained with H X 400

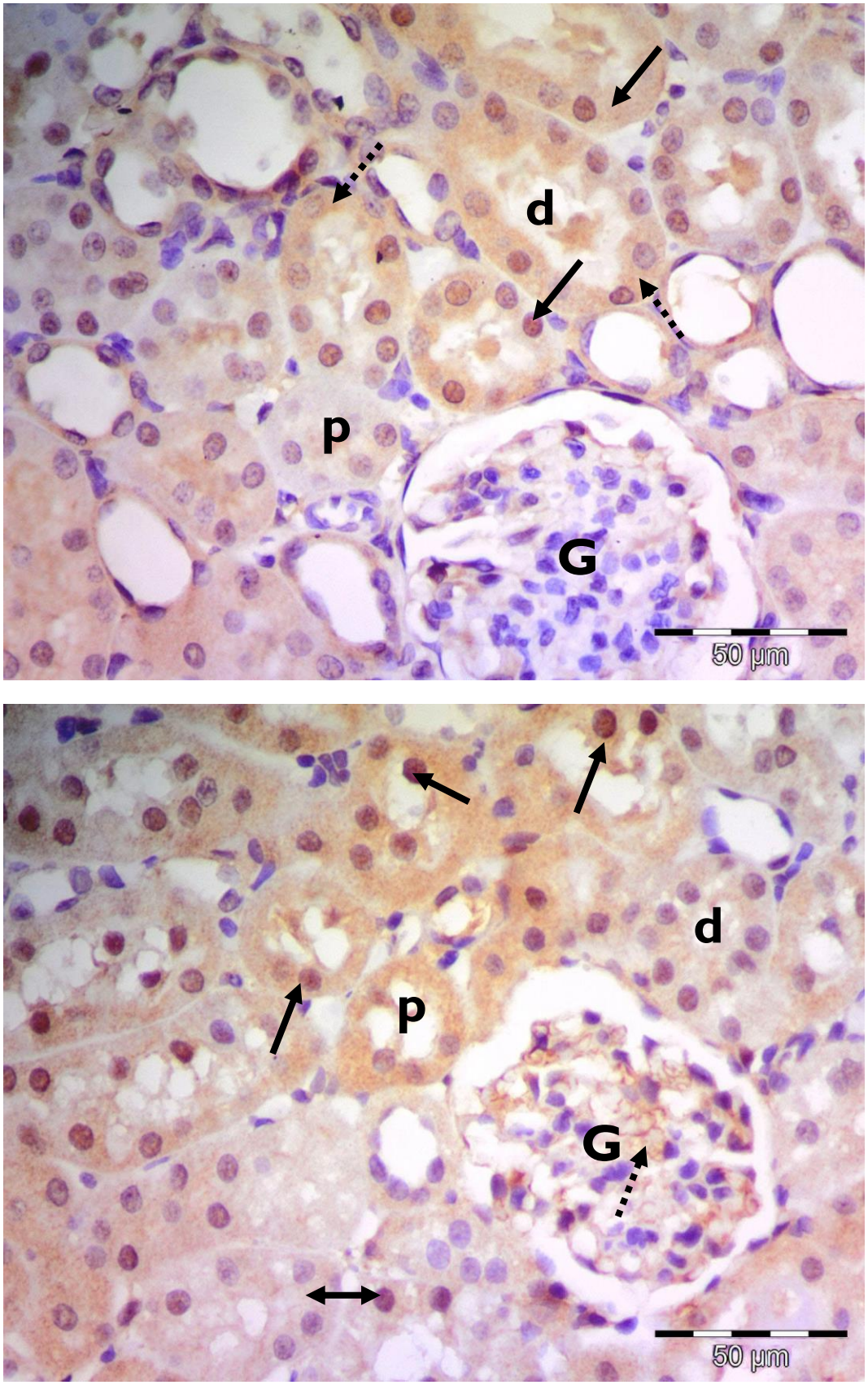

Fig.25: Representative photomicrographs of a section in rat kidney of **LIR group** showing positive cytoplasmic (dashed arrow), nuclear (arrows) and both cytoplasmic and nuclear (double headed arrows) caspase-3 immune reactivity in the glomerular (G), PCT (p) and DCT (d) cells.
Caspase-3 Immunohistochemistry counterstained with H X 400

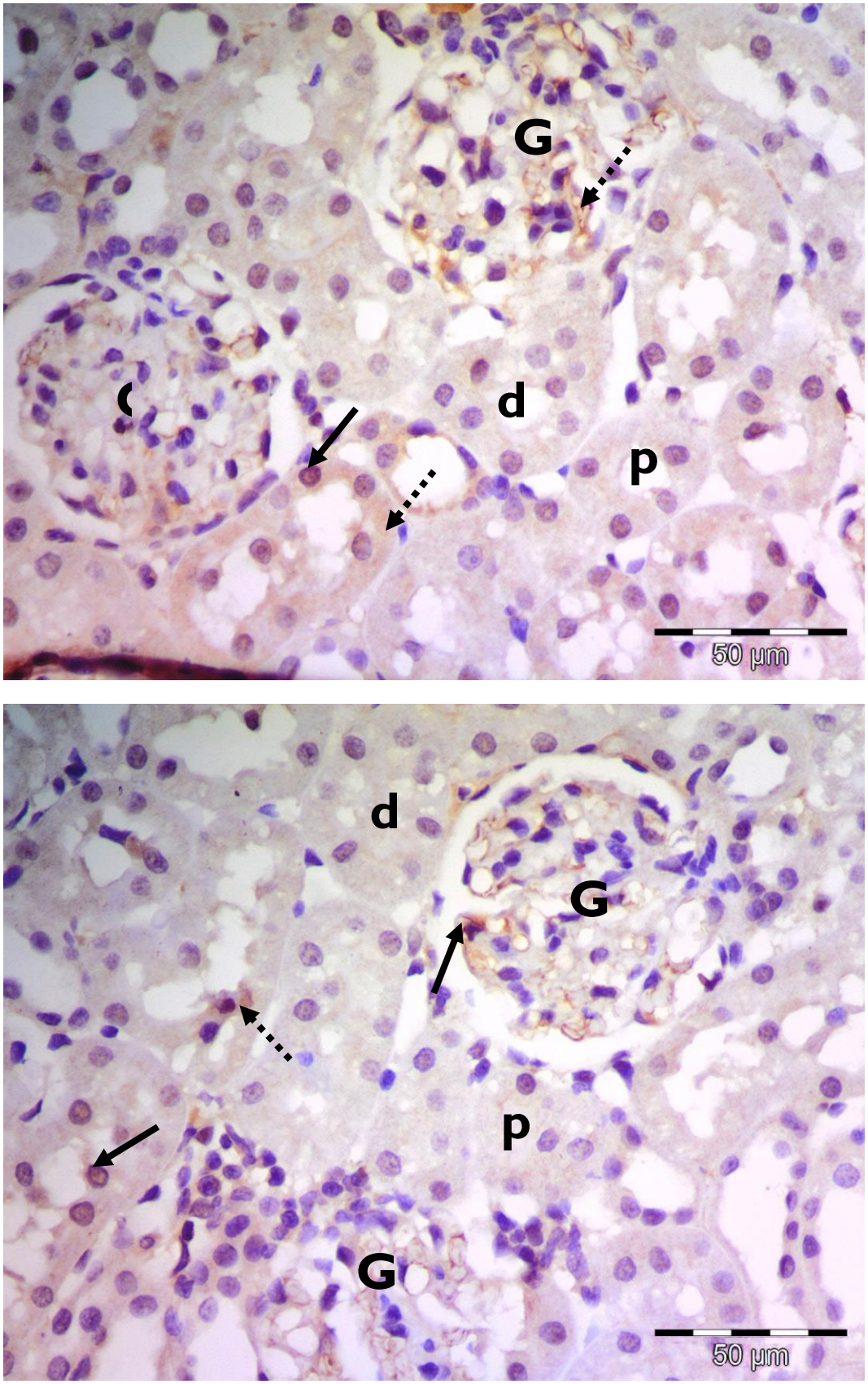

Fig.26: A representative photomicrograph of a section in rat kidney of **LIR+ naloxone group** showing mild caspase-3 positive cytoplasmic (dashed arrow) and nuclear (arrows) expression in some glomerular (G) and tubular cells
Caspase-3 Immunohistochemistry counter stain H x400